Universitatea
Transilvania
din Brașov

INTERDISCIPLINARY DOCTORAL SCHOOL

Faculty of Silviculture Forest Engineering

Florinel CAPALB

Utilization of integrated remote sensing data acquired by active and passive sensors for estimating tree dendrometric characteristics and analyzing radial growth in forest stands of the Western Southern Carpathians

SUMMARY

Scientific Supervisor

Acad. Nicolae Ovidiu BADEA

BRAȘOV, 2026

TABLE OF CONTENTS

LIST OF ABBREVIATION

UAV	Unmanned Aerial Vehicles
LiDAR	Light Detection and Ranging
ALS	Airborne Laser Scanning
TLS	Terrestrial Laser Scanning
dbh	Diameter at Breast Height (measured at 1.3 m above ground)
h	Tree Height
MLS	Mobile Laser Scanning
AI	Artificial Intelligence
3D	Three-Dimensional
B.E.	Experimental Base
UP	Production Unit
UAT	Administrative-Territorial Units
EEA	European Environment Agency
RS	Systematic Network
SP	Permanent Sample Plot
SPP	Permanent Sample Plot Area
N_i	Identifier of the "i" Sample Plot
C_1; C_2	Identifiers of Permanent Sample Plot Center
GPS	Global Positioning System
h_c	Crown Height
SfM	Structure from Motion
N; E; S; V	Cardinal Directions: North, East, South, West
.rwl	Tucson Format Files
CI	Competition Indices
x,y	Cartesian Coordinates
N	Total Number of Reference Trees
TP	Number of Correctly Detected Trees (matching trees)
FN	Number of Reference Trees Not Detected
FP	Number of Trees Segmented from Point Clouds
C	Detection Accuracy
e_{om}	Omission Error
e_{com}	Commission Error
RMSE	Root Mean Square Error
RRMSE	Relative Root Mean Square Error
MAE	Mean Absolute Error
R^2	Coefficient of Determination
TRW	Tree Ring Width
BAI	Basal Area Increment
CSV	Crown Structure Variables Derived from Point Clouds
εi	Residual Error
VIF	Variance Inflation Factor
AIC; BIC	Statistical Criteria Used for Model Selection

network FA	Beech Research Network
$\overline{dbh}$	Mean Diameter at Breast Height
$\bar{h}$	Mean Tree Height
network MO	Spruce Research Network
network AM	Mixed Research Network (spruce, beech)
sd	Standard Deviation
$\overline{CBH}$	Mean Crown Base Height
$\overline{CPA}$	Mean Crown Projection Area
FA	Beech Species (FA)
MO	Spruce Species (MO)
s%	Coefficient of Variation
SP 6; SP 84; SP 91; SP 28; SP 26; SP 39; SP 38; SP 24	Permanent Sample Plots from Inventory Networks
r	Pearson Correlation Coefficient
r^2	Correlation Ratio
SPP 232	Permanent Sample Plot Area from the AM Research Network
χ^2	Chi-Square Goodness-of-Fit Test
Wilcoxon	Rank-Based Statistical Analysis
Q1	Lower Quartile
Q3	Upper Quartile
CD	Crown Diameter
HCB	Height to Crown Base
CL	Crown Length
asim	Crown Asymmetry
R_{max}	Maximum Crown Radius of the Tree
R^2	Coefficient of Determination
CCC	Lin's Concordance Correlation Coefficient
Bias	Systematic Error
df	Degrees of Freedom
KS	Kolmogorov – Smirnov Test
ANOVA	Analysis of Variance
AIC	Akaike Information Criterion
cvTRW	Coefficient of Variation of Tree Ring Width
CR	Crown Radius
CSLC	Crown Shape Length Coefficient
rețea	Statistical Inventory Network (AM, FA, MO)
CLz	Standardized Crown Length, m
CDz	Standardized Crown Diameter, m
CIz	Standardized Competition Index
TRWz	Standardized Tree Ring Width
SEM	Structural Equation Model
CFI	Comparative Fit Index
SRMR	Standardized Root Mean Square Residual

year	Observation Year
tree_id	Tree Identification Number
R^2_m	Marginal Coefficient of Determination
R^2_c	Conditional Coefficient of Determination

PREFACE

In recent decades, the development of remote sensing technologies and the increasing accessibility of geospatial data have led to significant changes in the way forest ecosystems are analyzed and monitored. The integration of data acquired through active and passive sensors enables the extraction of detailed information regarding stand structure and tree dendrometric characteristics, contributing to the development of modern methods for the assessment and monitoring of forest ecosystems.

The doctoral thesis entitled *" Utilization of integrated remote sensing data acquired by active and passive sensors for estimating tree dendrometric characteristics and analyzing radial growth in forest stands of the Western Southern Carpathians"* falls within this scientific research direction and aims to apply integrated analytical methods based on the use of data obtained through terrestrial laser scanning, UAV (Unmanned Aerial Vehicle) platforms, and measurements carried out during conventional forest inventories. The conducted research focused on determining the dendrometric characteristics of trees and their crowns, as well as evaluating the relationships between stand structure, competition intensity, and tree radial growth.

The accomplishment of these objectives would not have been possible without the constant support of my scientific supervisor, Acad. Nicolae Ovidiu Badea, to whom I express my deepest gratitude and sincere appreciation for his effort, support, and patience demonstrated through his competent and continuous guidance throughout the entire process of developing and completing this doctoral thesis, as well as for his essential contribution to my professional development.

I would also like to express my gratitude to Prof. Dr. Eng. Iosif Vorovencii, Prof. Dr. Eng. Gheorghe Marian Tudoran, and Senior Researcher I Dr. Eng. Bogdan Apostol for their advice, observations, and recommendations provided during the presentation of the scientific reports and throughout the preparation of the thesis.

I express my sincere appreciation and gratitude to my colleagues from the National Institute for Research and Development in Forestry "Marin Drăcea" for their support and encouragement throughout the development of this doctoral thesis, especially to Dr. Eng. Marius Petrila, Dr. Eng. Adrian Lorenț, and geographer Cristiana Marcu. I also respectfully thank Dr. Eng. Ștefan Leca, Dr. Eng. Alexandru Dobre, Eng. Cristian Angheluș, Eng. Gabriel Nedea, Eng. Costin Barbu, and technician Răducu Stănculeanu for their support in the research activities carried out within this study. Special thanks are also addressed to Dr. Eng. Șerban Chivulescu for his support, suggestions, and observations provided during the preparation and development of the doctoral thesis.

Last but not least, I would like to thank my family, especially my wife Claudia, for her moral support, patience, and understanding throughout the entire period of preparing this doctoral thesis. A special thought is dedicated to my mother, Victoria, who would have experienced with profound emotion the accomplishment of this academic endeavor.

This list of appreciation and thanks undoubtedly remains incomplete. I express my gratitude to all those who, although not specifically mentioned in these lines, supported me and stood by me, directly or indirectly, throughout the preparation of this doctoral thesis.

1. INTRODUCTION

In the last two decades, the role of remote sensing in forestry research has expanded considerably, remote sensing data being increasingly used to extract and analyze tree and forest stand characteristics, both through the use of active sensors (Calders et al. 2020; Compeán-Aguirre et al. 2024; Corte et al. 2020; Dubayah et al. 2020; Mîzgaciu et al. 2025; Picos et al. 2020; Wallace et al. 2016) and passive sensors (Ball et al. 2023; Beloiu et al. 2023; Onishi and Ise 2021). Among the platforms used for the acquisition of these data, an increasingly important role is played by Unmanned Aerial Vehicles (UAVs), equipped with LiDAR systems, optical cameras, or multispectral sensors, which involve reduced operational costs (Onishi and Ise 2021), but are limited in terms of the size of the covered area, as well as payload capacity, which constrains the type and weight of the sensors that can be integrated.

Remote sensing based on the use of high-resolution data acquired through active and passive sensors, resulting from Airborne Laser Scanning (ALS), Terrestrial Laser Scanning (TLS), as well as UAV-based acquisitions, represents an area of intensive research for the characterization of forest ecosystems (Calders et al. 2020; Dobre et al. 2021; Shang et al. 2019). Although ALS systems are efficient for covering extensive areas, they encounter difficulties in the accurate detection of forest vegetation at ground level and do not allow a detailed representation of tree stems (So et al. 2025). In this context, TLS stands out as a technology capable of generating three-dimensional point clouds (Fan et al. 2020; He et al. 2025), which provide detailed information for the characterization of forest structure (Griese, Ritzert and Nölke 2025; Pascu et al. 2019; Wang et al. 2021), especially beneath the forest canopy (He et al. 2025; White et al. 2016; Zhou et al. 2023). However, the use of terrestrial laser scanning presents limitations when applied over large areas, due to its reduced mobility and static nature. At the same time, it should be noted that the occlusion effect (the partial or complete obstruction of target surfaces by vegetation elements such as leaves, branches, and stems) (Jiang et al. 2021) represents one of the main limitations of its application in the forestry field (Mîzgaciu et al. 2025).

On the other hand, images acquired using UAVs equipped with optical or multispectral cameras allow, through photogrammetric techniques, the generation of digital surface models and canopy models, facilitating the description of canopy structure and the identification of individual trees or tree crowns (Griese, Ritzert and Nölke 2025). Compared to TLS, UAV-based data acquisition enables the generation of point clouds over larger areas, although with lower point densities (Chen et al. 2024). When used independently, both TLS and UAV systems lead to significant occlusion effects; however, TLS tends to underestimate tree tops due to its bottom-up perspective (Terryn et al. 2022), thus requiring complementary measurements acquired above the forest canopy (Schneider et al. 2019).

The potential of TLS for forest monitoring was first highlighted in the early 2000s. Initially, applications focused on measuring trees and their structural components, as well as tree diameter at breast height (dbh) (Wezyk et al. 2007) and total tree height (h) (García et al. 2011), eventually evolving toward the estimation of tree volume (Abegg et al. 2023; Pitkänen et al. 2021), with the aim of improving aboveground biomass estimation (Demol et al. 2022; Liang et al. 2016), as well as determining tree position within forest stands (Bienert et al. 2018; Bogdanovich et al. 2021; Maas et al. 2008; Olofsson, Holmgren and Olsson 2014; Srinivasan et al. 2015). In addition, considerable progress has also been made in the determination of the three-dimensional crown structure (Han and Sánchez-Azofeifa 2022; Zhu, Kleinn and Nölke 2020), thus providing a detailed perspective on forest vegetation.

Moreover, terrestrial laser scanning provides extensive possibilities for representing crown shape with a high degree of precision (Calders et al. 2020; Olivier, Robert and Fournier 2016), facilitating access to crown characteristics (Pretzsch 2021), thereby creating the necessary conditions for explaining the relationship between crown shape and annual ring width (Ahmed and Pretzsch 2023; Kröner et al. 2024). Similar to annual rings, crown shape preserves information regarding the previous development of trees. Crown morphology may be influenced by abiotic factors, such as prevailing winds or terrain slope (Perles-Garcia et al. 2022). However, competition among trees (competition at crown level) represents the main factor determining crown shape. In general, tree crowns tend to develop in the opposite direction of dominant trees or their nearest neighbors, occupying the gaps within the canopy (Purves, Lichstein and Pacala 2007).

As a response to environmental conditions and competition, each tree develops its own crown (Penanhoat et al. 2024), through which it optimizes access to light and other resources, thereby maximizing its growth potential (Jucker et al. 2025). Crown shape and branch distribution are highly dynamic traits that enable trees to adapt to variations in environmental conditions. In this way, tree crowns reflect the outcome of complex interactions between growth processes and environmental conditions, which directly influence current tree growth (Bayer, Seifert and Pretzsch 2013; Kröner et al. 2024).

With the widespread use of terrestrial and airborne LiDAR data, as well as point clouds acquired using UAVs, research on crown shape and three-dimensional crown structure has intensified (Arrizza et al. 2024; Weiser et al. 2022). At the international level, numerous studies have demonstrated the potential of TLS to accurately describe forest stand structure and to complement and improve the information obtained through traditional forest inventories (Holvoet et al. 2025).

Subsequently, the integration of TLS and ALS remote sensing data was used to accurately estimate biomass and carbon stocks, by combining tree-level information with the extensive spatial coverage provided by airborne laser scanning (Bazezew, Hussin and Kloosterman 2018; Giannetti et al. 2018). In parallel, recent studies have used UAVs equipped with high-resolution optical cameras or LiDAR systems to describe canopy structure, canopy gaps, as well as the stratification of tree crowns (Mohan et al. 2017; Nasiri et al. 2021; Solano et al. 2022).

In the context of growth modeling, a current research direction involves the use of crown parameters derived from remote sensing data in growth models (Ahmed and Pretzsch 2023). Recent studies have shown that the inclusion of such parameters (crown length, crown height, crown projection area, etc.) can significantly improve the accuracy of growth models (Ahmed and Pretzsch 2023; Pretzsch 2021). Thus, the relationships between crown shape derived from TLS data and annual ring width have been investigated for several forest species, highlighting the fact that the current crown shape can explain both radial growth variation and tree response to stress factors (Ahmed et al. 2025; Kröner et al. 2024).

In Romania, the use of remote sensing technologies for the characterization of forest structure and dynamics has experienced rapid development. The first TLS applications focused on comparing modern data acquisition methods with traditional forest inventory methods (Apostol et al. 2018), later followed by studies using terrestrial laser scanning for the estimation of forest stand structural characteristics and the derivation of structural indices at plot level (Pascu et al. 2019, 2020).

In parallel with the consolidation of TLS applications, automated workflows integrating Mobile Laser Scanning (MLS) and Artificial Intelligence (AI) platforms have also been developed (Wielgosz et al. 2024). In this context, Niță (2021) tested and validated an automated workflow for the processing of 3D point clouds, focused on individual tree segmentation, obtaining a high segmentation accuracy.

The integration of TLS and ALS has been applied in the assessment of forest ecosystem services by correlating structural parameters derived from point clouds with ecological indicators (Dobre et al. 2021). More recently, the use of remote sensing data acquired through passive sensors has enabled the development of national-scale forest characteristic mapping models based on satellite imagery (Dinca et al. 2017; Vorovencii 2024) and machine learning algorithms (Keskes et al. 2025), while applied research has demonstrated the potential of UAV platforms equipped with LiDAR systems or optical cameras for the estimation of dendrometric parameters and forest stand structure in various forest types from Romania (Mîzgaciu et al. 2025; Tudoran 2022).

The doctoral thesis aims to use remote sensing data acquired through active and passive sensors for the development of tree- and stand-level growth models calibrated for forest stands located in the western part of the Southern Carpathians. For this purpose, the research focused on estimating the structural characteristics of trees and forest stands through the application of remote sensing techniques and on obtaining dendrometric parameters through the processing and segmentation of point clouds. The validation of the results was carried out through a comparative analysis of the performance of the growth models developed based on remote sensing data in relation to the information obtained during field tree inventories.

2. AIMS AND OBJECTIVES OF THE RESEARCH

2.1. AIMS OF THE RESEARCH

The research conducted during the preparation of the doctoral thesis aimed at the scientific substantiation and application of remote sensing techniques regarding the integrated use of data acquired through active and passive sensors together with field measurements carried out through inventories in permanent sample plots, for the determination of tree dendrometric characteristics and crown characteristics, as well as for the analysis of radial growth in forest stands from the western part of the Southern Carpathians.

2.2. OBJECTIVES OF THE RESEARCH

In order to achieve the proposed aim, the following specific objectives were pursued:

- estimating dimensional characteristics of trees and their crowns by using integrated data obtained through remote sensing techniques through field measurements;
- development of tree radial growth models based on crown characteristics and stand-level competition indices obtained through remote sensing;
- analysis of the radial growth of trees and forest stands developed on the basis of data and information obtained through remote sensing techniques in relation to those obtained from measurements carried out during field inventories.

3. METHODOLOGY AND RESEARCH MATERIAL

3.1. RESEARCH LOCATION

The research was carried out in pure beech (FA) and spruce (MO) stands, as well as in mixed spruce–beech stands (AM), located in the western part of the Southern Carpathians, more precisely in the Țarcu Mountains, situated in the north-western part of the Retezat-Godeanu mountain group, a mountainous unit with altitudes exceeding 2100 m. More specifically, the area selected for conducting this research is located within the Caransebeș Experimental Base (B.E.), in Production Unit (UP) VI Cuntu (Figure 3.1).

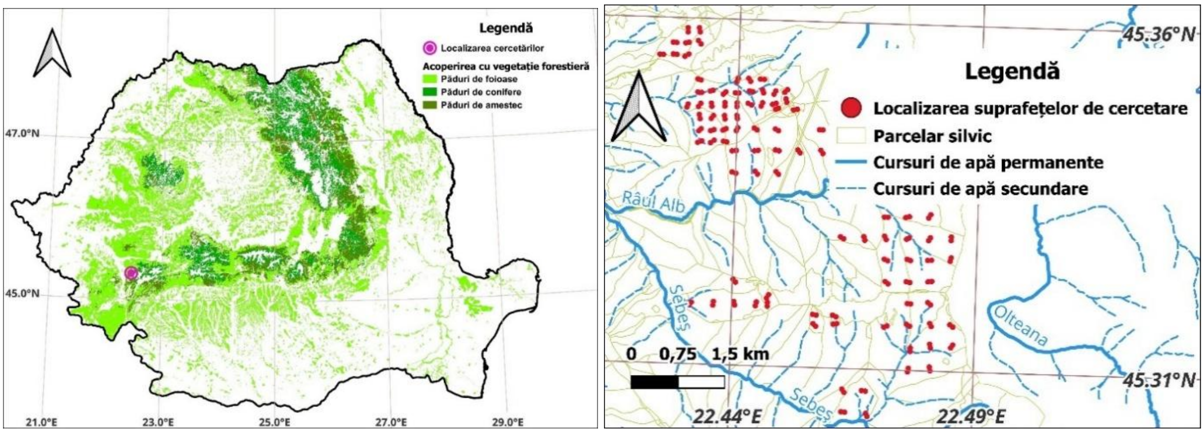

Figure 3.1 *– Location of the research areas in relation to the distribution of forest vegetation cover at national level. The cartographic background represents forest vegetation classes derived from CORINE Land Cover* (European Environmnet Agency (EEA) 2020)*, namely broad-leaved forests (class 311), coniferous forests (class 312), and mixed forests (class 313). The points/areas (red color) indicate the location of statistical inventory network.*

3.2. RESEARCH MATERIAL

In order to characterize the forest stands within the research area, a non-systematic statistical research network was designed, with the purpose of providing a biometric characterization of even-aged or relatively even-aged beech and spruce stands, as well as mixed spruce–beech stands, within Production Unit (UP) VI Cuntu. The reason why the research network is non-systematic at the level of the entire study area is that it was not uniformly designed according to a single grid applied across the whole research area, but rather resulted from the combination of three systematic statistical networks (RS), designed in relation to species (beech, spruce), composition (pure stands – beech, spruce; mixed spruce–beech stands), and age structure (even-aged or relatively even-aged stands).

The design of the systematic statistical networks, namely the establishment of the optimal number of permanent sample plots (SP) and the distances between them, was carried out using information regarding the coefficient of variation of stand volume calculated based on the data included in the forest management plan of Production Unit (UP) VI Cuntu (Caransebeș Experimental Base, 2016 edition). The non-systematic statistical inventory network, intended for the inventory of even-aged or relatively even-aged beech, spruce, and mixed stands, consisted of three systematic networks with variable density, totaling 96 sample plots (Table 3.1). Based on the resulting number of sample plots and the established distances between them, permanent sample plots area (SPP) were established in the field.

Table 3.1 – *Number of sample plots corresponding to the statistical inventory networks*

Inventory network	Density	Number of sample plots
beech (FA)	200 m x 200 m	38
spruce (MO)	150 m x 150 m	10
Mixed forests - spruce, beech (AM)	350 m x 350 m	48
TOTAL		96

Each permanent sample plot (SP) included two permanent sample plots area (SPP), circular in shape, with a radius of 12.62 m (surface area of 500 m²), located at a distance of 30 m from the center of the permanent sample plot, along the E–W direction on flat terrain and along the contour line on sloped terrain. In order to facilitate subsequent inventories, the center of the sample plot, as well as the centers of the two SPP, were marked using metal markers (20 cm in length), completely buried in the ground, as well as wooden reference stakes with the upper end positioned approximately 30 cm above the ground surface and highlighted with white paint (Figure 3.2).

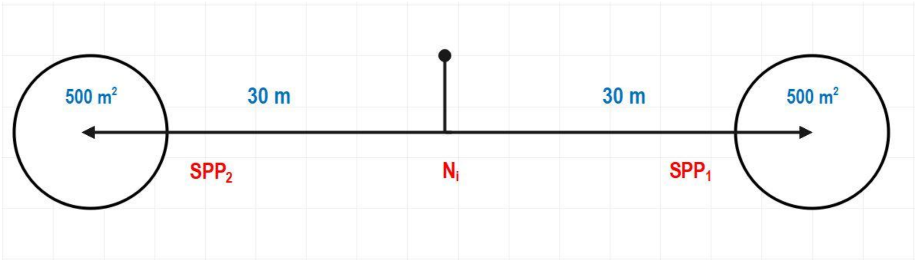

Figure 3.2 – *Location of the permanent sample plots area ($SPP_{1,2}$) in relation to the center of the plot (N_i).*

Within each statistical network, tree inventory was carried out in each permanent sample plot area (SPP) using the standing tree inventory method (Badea, 2013). All trees with a diameter at breast height (dbh) greater than 60 mm were inventoried. During the inventory, conducted in 2020, the following characteristics were determined and recorded in the field sheets for each tree: species, diameter at breast height (dbh), total height (h), crown height (hc), cenotic position (Kraft class), as well as descriptive information regarding vitality and damage status, specified in the specialized literature (Badea, 2008, 2013; Chivulescu et al. 2020).

Diameter at breast height measurements were carried out using a forestry caliper graduated in millimeters, in accordance with the established methodology (Giurgiu 1979). The point of application of the forestry caliper on the stem was marked with white paint using a "T" sign, which, on flat terrain, was placed on the side facing the center of the permanent sample plot area (SPP) in order to facilitate subsequent remeasurements, while on sloped terrain it was marked on the uphill side of the tree. In the case of trees with diameters exceeding the maximum opening of the caliper, circumference was measured in millimeters, following the same uphill positioning rule on sloped terrain (Badea, 2013; Chivulescu et al. 2020).

The total tree height and crown height were measured using the Vertex IV ultrasonic hypsometer. The sociological position of the trees was estimated in the field through visual assessment, using a classification system specific to even-aged and single-layered forest stands (Badea, 2013; Pikiński et al. 2021).

Tree position and crown projection were determined using the FieldMap system, in accordance with a precise methodology (Petrila et al. 2012). Each inventoried tree was assigned a unique identification number through the application of a numbered tag, in order to ensure the comparability of the data obtained through the conventional inventory with those subsequently derived from terrestrial laser scanning (TLS).

Within the permanent sample plots area (SPP), specific measurements were carried out in 2021 using a static terrestrial laser scanner, FARO 3D X130 HDR model (Apostol et al. 2018). This equipment belongs to the class of phase-shift[1] scanners (FARO Technologies Inc 2019), being designed for scanning applications at short and medium distances and providing high measurement accuracy, suitable for the three-dimensional characterization of forest stand structure (Apostol et al. 2018).

Within each SPP, TLS measurements were carried out by establishing four scan positions: the first position was located at the center of the SPP, the second toward the north, the third at 120° relative to the north direction, and the last at 240° relative to the north direction. The TLS scan positions, except for the one located at the center of the SPP, were positioned at a distance of 15 m from the center of the permanent sample plot. In order to achieve the automatic coregistration of the point clouds obtained from the scans, seven spherical targets uniformly distributed within the plot were installed (Figure 3.3).

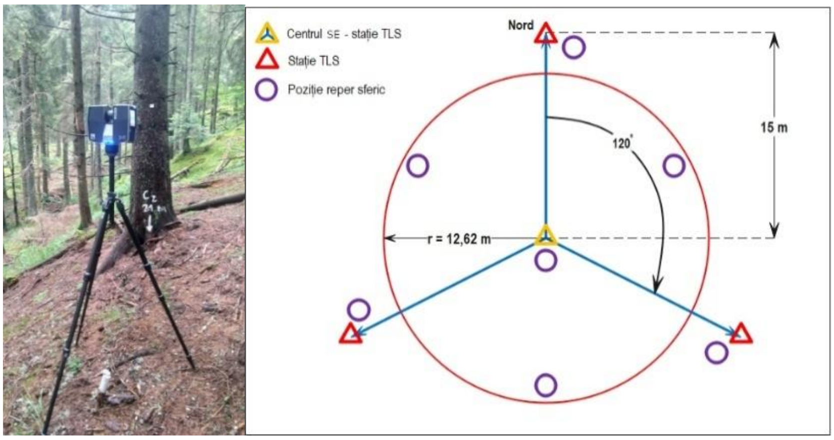

Figure 3.3 *– Location of TLS station in relation to the scanned sample surface*

At the same time, photogrammetric flights were carried out within each sample plot (SP) using a DJI Mavic 2 Enterprise Dual Unmanned Aerial Vehicle (UAV). The data and information obtained following these flights were processed using *Agisoft Metashape Professional* software (Agisoft LLC 2021). By applying the *Structure from Motion* (SfM) technique, natural color orthophoto images (RGB), as well as high-density point clouds describing the three-dimensional canopy structure, were generated (Iglhaut et al. 2019). The obtained point clouds were clipped using a 10 m buffer area outside the boundary of each permanent sample plot (SPP), so that trees located at the edge of the plots were fully represented.

[1] operates by measuring the phase difference between the emitted and the reflected wave

This step aimed to ensure comparability between the UAV and TLS datasets and to reduce the risk of underestimating tree crowns as a result of clipping at the SPP boundary.

At once, in order to determine tree-level radial growth, increment cores were collected in 2024 using a Pressler increment borer from a sample of 2–3 standing trees belonging to the main species (beech, spruce), representative for each diameter class and located within a 10 m wide buffer zone situated outside each permanent sample plot (Badea 2013).

After extraction, the increment cores were dried, mounted on wooden supports, and subsequently sanded progressively using abrasive belts with increasingly finer grain sizes (200–800), so that the annual rings became clearly visible and easier to identify. Subsequently, the samples were scanned at high resolution (1200 dpi), and annual ring width was measured using the CooRecorder software application (v.7.4) (Collazos Fernández and Rubiales 2025). The growth series for each tree was dated through visual examination, and the resulting values were exported and archived in *Tucson* format files *(.rwl).*

3.3. DATA PROCESSING AND STATISTICAL ANALYSIS

The analysis and characterization of the structure of the inventoried forest stands were carried out by comparing the dendrometric characteristics derived from point clouds with the values obtained through field-based forest inventories, both at tree level and at permanent sample plot (SPP) level. The information obtained in the field represented the reference dataset for dendrometric characteristics (diameter at breast height, total height, etc.), while the characteristics derived from point cloud processing were treated as estimates subject to validation through comparison.

In order to facilitate the extraction of tree attributes, a series of preprocessing steps were carried out, namely the coregistration of point clouds obtained from terrestrial laser scanning and UAV acquisitions, noise removal, and semantic segmentation of point clouds (Wielgosz et al. 2024). The coregistration of the point clouds was performed using the R software environment (Posit team 2025), through the use of the *lidRalignment* package (Roussel 2025), dedicated to the automatic alignment of point clouds originating from different sources. For the segmentation of individual trees, the resulting point clouds were processed through a fully automated workflow that uses point clouds as input data, identifies the points belonging to trees, and groups them into individual trees (Henrich et al. 2024).

Individual tree characteristics, such as diameter at breast height (dbh), tree height, and crown projection, were obtained from the point clouds resulting from the segmentation process, through the use of the *ITSMe* package (Terryn et al. 2023), which enables the estimation of individual tree characteristics based on point clouds.

The analysis of competition relationships (determination of competition indices) at tree level was carried out using the *TreeCompR* package (Rieder et al. 2024), which provides a solution for evaluating competition among trees and allows the comparison of multiple competition indices (CI) depending on the type of available data. In the case of the approach based on tree inventory data, *TreeCompR* can process datasets containing tree coordinates (x, y) and at least one variable such as diameter at breast height (dbh) or tree height (h). These data may originate either from field-based tree inventories or from results obtained through individual tree segmentation.

The evaluation of individual tree segmentation performance was carried out by comparison with the trees identified during the field inventory. For this purpose, the trees inventoried in the field were considered the reference dataset, while the trees resulting from point cloud segmentation were considered the prediction dataset. For each SPP, the correspondence between the two datasets was achieved by establishing pairs of inventoried tree–segmented tree pairs, so that each reference tree was assigned at most one segmented tree. For each SPP, the following were defined: *N* represents the total number of reference trees, *TP* the number of correctly detected trees (matching trees), FN the number of reference trees that were not detected, *FP* the number of trees segmented from the point clouds that do not correspond to any reference tree, while the sum of the correctly detected trees (TP) and the trees segmented from the point clouds that do not correspond to any reference tree (FP) represents the total number of trees segmented from the point clouds (Xiang et al. 2024).

Following the preprocessing stages, individual tree segmentation, and estimation of dendrometric characteristics, the accuracy of the estimates derived from the point clouds was evaluated by comparison with the measurements obtained through forest stand inventories, considered as reference data. The differences between estimated and measured values were quantified using standardized statistical error indicators, namely Root Mean Square Error (RMSE), Relative Root Mean Square Error (RRMSE), Mean Absolute Error (MAE), and the coefficient of determination (R^2), calculated separately for each analyzed attribute. All statistical analyses were implemented in the R software environment (Posit team 2025).

With regard to the verification of increment core cross-dating quality, this was carried out using the COFECHA software application (Labrecque-Foy et al. 2023; Zhang et al. 2024). The analysis and graphical representation of the dendrochronological series were performed using the R software environment (Posit team 2025), through the use of the *dplR* (Bunn 2008) and *detrendeR* (Campelo, García-González and Nabais 2012) packages, for a common period including at least five samples, thus obtaining validated dendrochronological series (TRW) aggregated by diameter classes, as well as basal area increment (BAI).

Since increment cores were collected from a sample of 2–3 trees located within the buffer zone of each sample plot (SP), the integration of dendrochronological series with the trees segmented from the point clouds was performed by diameter classes. Thus, for each diameter class, an average radial growth and an average basal area increment were calculated.

For modeling radial growth in relation to crown characteristics (crown diameter, crown length, crown base height), a parametric model (1) was used, in which the dendrochronological response was explained through a set of structural variables derived from point clouds (CSV). At the same time, the parametric model was defined so as to describe growth in relation to crown structure:

$$TRW_i = \beta_0 + \sum_{p=1}^{P} \beta_p CSV_{p,i} + \varepsilon_i \qquad (1)$$

where:
TRW_i represents ring width, mm;
$CSV_{p,i}$ - crown variables derived from point clouds;
ε_i - residual error.

Subsequently, in order to evaluate the influence of competition on tree radial growth, the model was extended by introducing competition indices (CI) as an additional variable:

$$TRW_i = \beta_0 + \sum_{p=1}^{P} \beta_p CSV_{p,i} + \beta_c CI_i + \varepsilon_i \quad (2)$$

where:
TRW_i represents ring width, mm;
$CSV_{p,i}$ - crown variables derived from point clouds;
CI_i - competition indices;
ε_i - residual error.

Prior to obtaining qualitative results and before model fitting, multicollinearity among crown characteristics was assessed through correlation analysis and evaluation of the Variance Inflation Factor (VIF) (Jacob and Varadharajan 2024; Salmerón-Gómez, García-García and García-Pérez 2025; Shrestha 2020), using the procedures implemented in the *car* package (Fox et al. 2021). In addition, in order to control local variation and observation dependency, mixed-effects models were also tested, in which the permanent sample plot (SP) was introduced as a random effect. It should also be noted that the mixed models were fitted using the *lme4* and *lmerTest* packages (Bates et al. 2015; Kuznetsova, Brockhoff and Christensen 2017), in order to ensure a high level of result reliability.

In parallel with the linear models used to evaluate the direct relationships between crown variables and radial growth, a Structural Equation Modeling (SEM) approach was also implemented in order to simultaneously analyze the direct and indirect relationships between crown characteristics and competition indices. This approach allows the evaluation of the mechanisms through which competition may influence radial growth both directly and indirectly, through modifications in crown characteristics.

The linear models were calibrated using crown variables derived from TLS point clouds and tree-level competition indices, while the selection and comparison of the fitted models were performed using the AIC and BIC information criteria, which take into account both model fit quality and model complexity (Chifunda, Kirigiti and Balan 2025; Zeferino et al. 2023).

The statistical analysis was performed using the R software environment, employing the base *stats* package (R Core Team 2025) for the Fligner–Killeen, Kruskal–Wallis (KW), Kolmogorov–Smirnov (KS), Likelihood Ratio Test (LRT), and Wilcoxon tests. In order to evaluate the degree of agreement, Lin's Concordance Correlation Coefficient (CCC) was used (Bornand et al. 2023), through the use of the *DescTools* package (Signorell A et al. 2024).

4. RESULTS OBTAINED

4.1. STATISTICAL INVENTORY OF INDIVIDUAL TREES AND STANDS WITHIN RESEARCH NETORKS

Through the specific inventory activities, a total of 96 permanent sample plots (SP), comprising 192 permanent sample areas (SPP), were surveyed. On this occasion, a total number of 6927 trees belonging to the investigated networks were inventoried. For the beech research network (FA), consisting of 38 sample plots, the calculated mean diameter at breast height ($\overline{\mathrm{dbh}}$) was 26.5 cm, while the calculated mean tree height ($\bar{h}$) was 22.4 m (Figure 4.1). Within the spruce research network (MO), consisting of 10 sample plots, ($\overline{\mathrm{dbh}}$) was 32.4 cm and ($\bar{h}$) was 23.8 m. In the mixed research network (AM), which included 48 permanent sample plots, it was found that, at species level, ($\overline{\mathrm{dbh}}$) was 24.8 cm for beech and 31.5 cm for spruce (Figure 4.1).

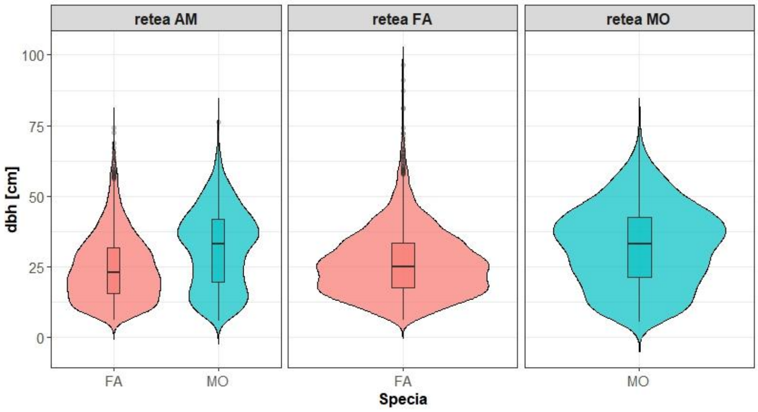

***Figure 4.1** – Distribution of the diameter at breast height (dbh) of inventoried trees, within the inventory networks.*

The analysis of the coefficients of variation (s%) of tree diameters within the permanent sample plots (SP) highlighted a relatively high variability in SP 6 (61.65%), SP 84 (60.11%), and SP 91 (60.06%), while the lowest values were recorded in SP 28 (21.49%), SP 26 (25.31%), and SP 39 (30.92%). Intermediate values of the coefficients of variation were recorded in SP 38 (35.94%), SP 22 (35.96%), and SP 24 (36.06%).

At network level, the coefficient of variation of tree diameters showed relatively similar values among the three analyzed networks (Table 4.1). In the AM network, which consisted of 48 permanent sample plots, the coefficient of variation of dbh was 44.3%. In the FA network (38 sample plots), the mean coefficient of variation of dbh recorded was 44.4%. The MO permanent network, comprising 10 sample plots, recorded the highest mean coefficient of variation of dbh, namely 48.4%. Statistical analysis did not reveal significant differences among the networks, as the Fligner–Killeen test did not indicate significant differences in the variation of the dbh coefficient of variation among them (χ^2 = 0.577, df = 2, p = 0.749), while the Kruskal–Wallis (KW) test also did not reveal significant differences in the distribution of the coefficient of variation among the networks (χ^2 = 2.507, df = 2, p = 0.285) (Figure 4.2).

Table 4.1 – Statistical parameters of tree diameter at breast height distribution at inventory network level

Inventory network	Number of permanent sample plot (SP)	Coefficient of variation [%]	Standard deviation [cm]	$s\%_{min}$ [%]	$s\%_{max}$ [%]
network AM	48	44,30	8,42	21,5	61,7
network FA	38	44,40	7,67	31,5	60,1
network MO	10	48,40	10,30	31,0	60,1

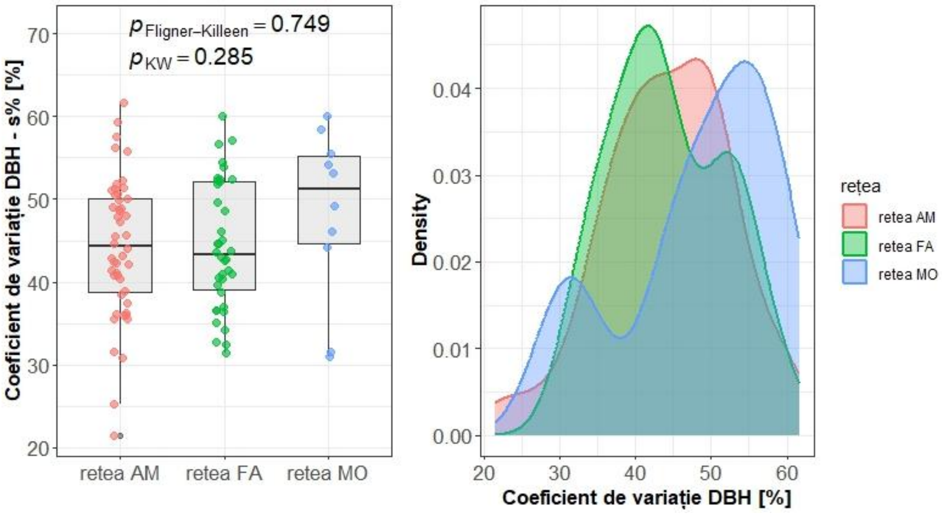

***Figure 4.2** – Distribution of the coefficient of variation of tree diameter at breast height at sample plot and statistical inventory network level.*

In order to test the homogeneity of dbh variance among the sample plots within each analyzed network, the nonparametric Fligner–Killeen test was applied. The obtained results revealed significant differences among sample plots for each of the three analyzed networks. In the mixed network (AM), the test indicated a pronounced heterogeneity of dbh variance (χ^2= 137.54, df = 47, p < 0.001). Similar results were also obtained for the FA (χ^2= 135.02, df = 37, p < 0.001) and MO (χ^2= 55.97, df = 9, p < 0.001) networks. The rejection of the null hypothesis (H_0) confirms that dbh dispersion differs significantly among permanent sample plots (SP), which required the homogenization of the system through the identification and grouping of SPs within each network into subpopulations with similar characteristics.

Thus, in the mixed network (AM), subpopulation A, consisting of 29 permanent sample plots (SP), presented a value at the significance threshold limit (χ^2= 41.17, df = 29, p = 0.051), while for subpopulation B (19 permanent sample plots) no significant differences were identified (χ^2= 12.77, df = 19, p = 0.804). Similarly, in the FA network (38 sample plots), no significant differences were identified either in subpopulation A (20 permanent sample plots, χ^2= 28.76, df = 19, p = 0.069) or in subpopulation B (18 permanent sample plots, χ^2= 14.99, df = 17, p = 0.595). In the spruce network (MO), consisting of 10 permanent sample plots, no significant differences were identified (χ^2= 10.85, df = 9, p = 0.144).

With regard to tree height, the coefficient of variation of tree height at network level showed relatively similar values among the three analyzed research networks (Table 4.4). In the AM network, consisting of 48 permanent sample plots, the coefficient of variation was 34.8%. In the FA network (which included 38 sample plots), the resulting coefficient of variation was 34.5%. The MO network (10 sample plots) recorded the highest coefficient of variation of tree height, namely 39.0%. Compared to the AM and FA networks, the MO network exhibited a slightly higher variability, but with a narrower variation range than that observed in the AM network. Statistical analysis did not reveal significant differences among the analyzed networks, as the Fligner–Killeen test did not indicate significant differences in the variation of the coefficient of variation of tree height among them (χ^2= 28.76, df = 19, p = 0.069), while the Kruskal–Wallis (KW) test did not reveal significant differences in the distribution of the coefficient of variation of tree height (Figure 4.3).

***Table 4.2** – Statistical parameters of tree height distribution at inventory network level*

Inventory network	Number of permanent sample plot (SP)	Coefficient of variation [%]	Standard deviation [m]	$s\%_{min}$ [%]	$s\%_{max}$ [%]
network AM	48	34,80	7,18	14,6	51,0
network FA	38	34,50	7,22	19,8	45,5
network MO	10	39,00	6,00	30,1	46,2

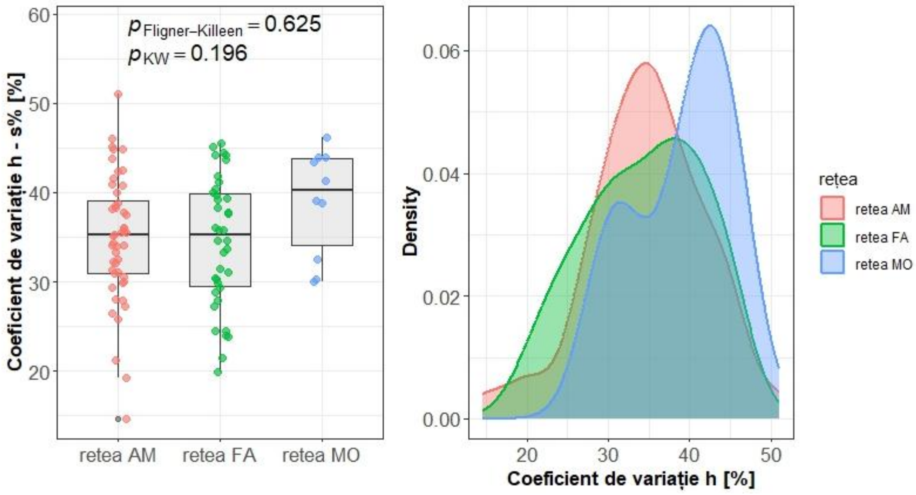

***Figure 4.3** – Distribution of the coefficient of variation of tree height at sample plot level in relation to the statistical inventory network.*

Within the forest stands belonging to the analyzed research networks, a predominance of trees with diameter at breast height (dbh) values ranging between 20 and 60 cm was observed. Depending on the inventory network, this category represents between 59% and 73% of the total number of trees. Moreover, trees with dbh values smaller than 20 cm account for between 22% and 40%, while trees with dbh values greater than 60 cm represent less than 3% of the total number of inventoried trees (Figure 4.4).

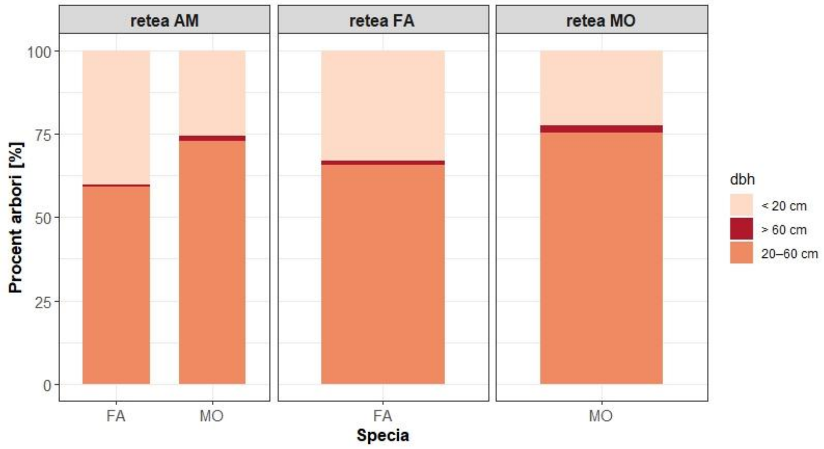

***Figure 4.4** – Relative proportion by diameter at breast height classes (<20 cm; 20 – 60 cm; >60 cm) at inventory network and species level.*

For the analysis of vertical structure within each network (AM, FA, MO), the tree heights measured in the sample plots were grouped into three intervals (<16 m, 16–32 m, and >32 m), their delimitation being established according to the distribution of mean heights corresponding to the positional classes (Kraft I–V) of the trees (Table 4.3). The obtained values highlight a grouping of trees belonging to Kraft positional classes IV and V below 16 m, those belonging to Kraft positional classes II and III within the 16–32 m interval, and trees from Kraft positional class I above 32 m.

***Table 4.3** – Tree height in relation to sociological position (Kraft classes) within the inventory networks*

Inventory network	Species	Height class [m]	Kraft classes	$\bar{h}$ [m]	Standard deviation [m]	$\overline{h_{min}}$ [m]	$\overline{h_{max}}$ [m]
network AM	beech	>32	I	34,0	3,36	26,5	41,9
		16 – 32	II, III	26,3	4,14	12,4	39,6
		<16	IV, V	14,2	4,89	2,1	30,7
	spruce	>32	I	33,5	3,11	22,0	44,0
		16 – 32	II, III	27,7	4,07	10,5	37,5
		<16	IV, V	13,2	5,51	2,1	34,3
network FA	beech	>32	I	32,4	3,32	21,5	39,7
		16 – 32	II, III	25,5	4,96	9,2	45,4
		<16	IV, V	13,5	5,98	1,4	31,5
network MO	spruce	>32	I	34,4	3,23	24,9	41,6
		16 – 32	II, III	27,2	4,62	14,9	35,1
		<16	IV, V	12,6	5,23	2,5	24,9

With regard to total tree height, the forest stands within the analyzed inventory networks were characterized by a predominance of trees with heights ranging between 16 and 32 m. Depending on the inventory network and species, this category represented between 46.6% and 66.8% of the total number of trees. Trees with heights lower than 16 m accounted for between 17.9% and 24.8%, while trees with total heights exceeding 32 m represented between 15.3% and 33.4% of the total number of inventoried trees (Figure 4.5).

In the AM network, for beech, 62.7% of the trees recorded heights between 16 and 32 m, while 17.9% exceeded 32 m. In the case of spruce within the same network, the distribution was more uniform: 46.6% of the trees fell within the 16–32 m interval, 24.8% had heights below 16 m, while 28.6% exceeded 32 m in height, highlighting a higher proportion of tall trees compared to beech (Figure 4.5, Figure 4.6).

In the FA network, 66.8% of the total number of trees had heights ranging between 16 and 32 m, while 15.3% exceeded 32 m, indicating a concentration of trees within the intermediate height classes and a relatively reduced proportion (15.3%) of trees taller than 32 m. Likewise, in the MO network, 46.7% of the total number of trees had heights between 16 m and 32 m, while 33.4% exceeded 32 m (Figure 4.5, Figure 4.6).

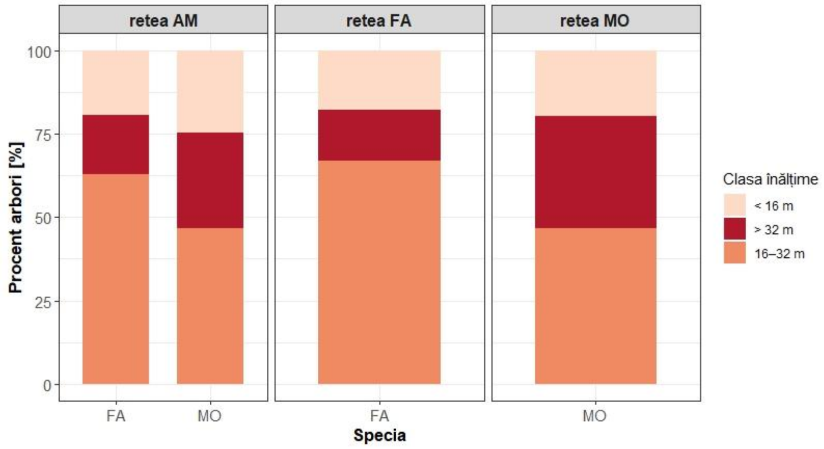

Figure 4.5 *– Relative proportion by height classes (<16 m, 16–32 m, >32 m) at inventory network and species level.*

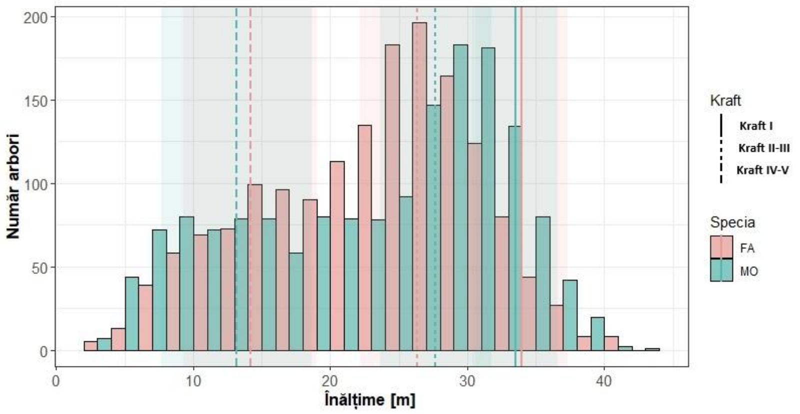

(a)

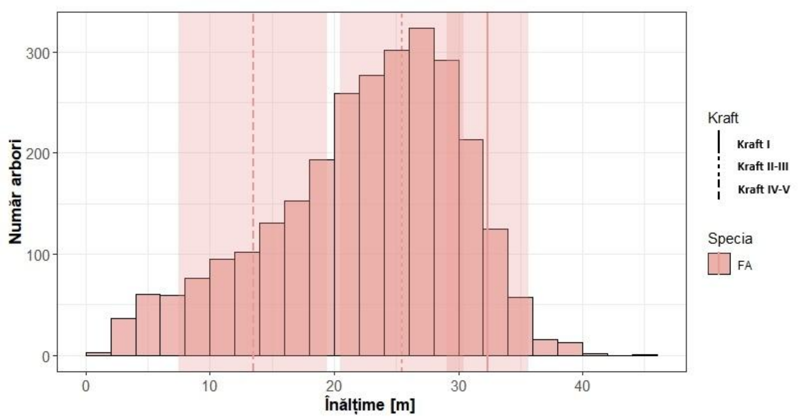

(b)

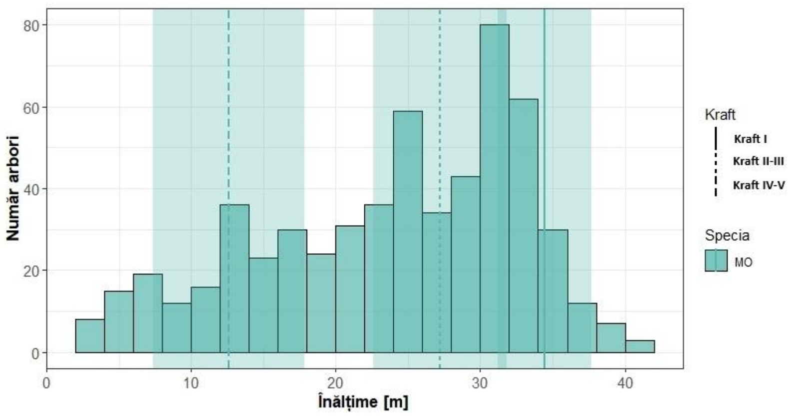

(c)

Figure 4.6 *– Distribution of trees by height classes (2m) at inventory network level: AM (a), FA (b), MO (c).*

For the analysis of the diameter at breast height – height relationship, height curves (h) in relation to tree diameter at breast height (dbh) were constructed based on the information obtained through the inventories (Figure 4.7). The strength of the correlation between the two dendrometric characteristics was evaluated using the Pearson correlation coefficient (r), as well as the correlation ratio (r^2).

The analysis of the relationship between diameter at breast height and tree height highlights a strong positive association between the two variables for all analyzed networks and species (Table 4.4). In the AM network, the correlation coefficient (r) was 0.781 for beech (r^2 = 0.772) and 0.906 for spruce (r^2 = 0.898).

For the network, respectively for beech, the correlation coefficient (r) was 0.692, while the value of the correlation ratio was 0.680. In the MO network, for spruce, the relationship was characterized by a higher intensity, with r = 0.825 and r^2 = 0.816.

Comparatively between species, the dbh–h relationship was consistently stronger for spruce than for beech, regardless of the network. In addition, the AM and MO networks showed higher correlation ratio values (r^2) compared to the FA network (Table 4.5).

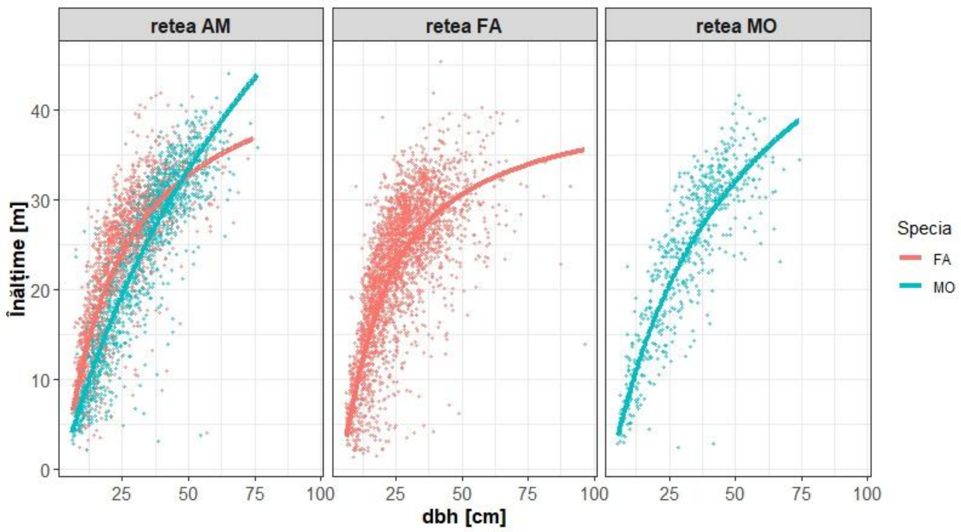

Figure 4.7 – Height curves at inventory network and species level: AM network, FA beech network, MO network.

Tabel 4.4 – Determination of coefficients of the regression equation of the form $\ln h = a_0 + a_1 \cdot d^{a_2}$ (Giurgiu, Decei & Draghiciu, 2004)

Inventory network	Species	Regression coefficients $\log h = a_0 + a_1 \cdot \log d + a_2 \cdot log^2 d$			Regression equation coefficients $\ln h = a_0 + a_1 \cdot d^{a_2}$		
		a_0	a_1	a_3	a_0	a_1	a_2
network AM	beech	-1,209	2,266	-0,273	3,749	-9,938	-0,922
	spruce	-2,751	2,772	-0,299	4.411	-9,451	-0,603
network FA	beech	-2,629	3,091	-0,397	3,595	-17,732	-1,173
network MO	spruce	-2,612	2,933	-0,351	3,792	-13,669	-0,970

Table 4.5 – Value of the correlation coefficients (r) and correlation ratios (r^2) between tree diameter at breast height and tree height

Inventory network	Species	Correlation coefficient (r)	Correlation ratio (r^2)
network AM	beech	0,781	0,772
	spruce	0,906	0,898
network FA	beech	0,692	0,680
network MO	spruce	0,825	0,816

4.2. TREE DENDROMETRIC CHARACTERISTICS DETERMINED VIA TERRESTRIAL LASER SCANNING AND UAV

The information obtained through field inventories constituted the reference dataset used for evaluating the accuracy of the estimates derived from terrestrial laser scanning (TLS). The permanent sample plots, each covering an area of 500 m^2, were entirely surveyed and scanned using terrestrial laser scanning (TLS). As a result, a total number of 768 scans were obtained (four scans for each permanent sample plot). Following the processing of the point clouds, a coregistered point cloud was obtained for each SPP (Figure 4.8), and statistical reports containing information regarding coregistration accuracy were subsequently generated.

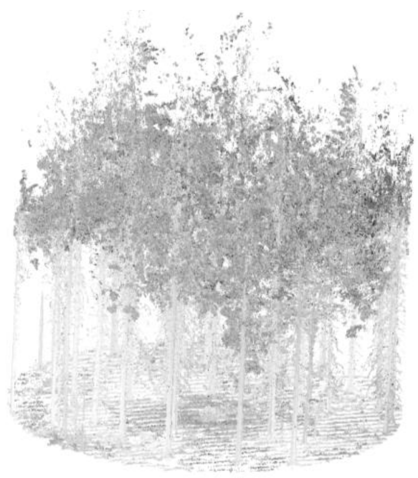

Figure 4.8 – *Three-dimensional point cloud obtained through terrestrial laser scanning (TLS) at the permanent sample plot (SPP) level (e.g., SPP 232).*

The analysis of coregistration errors highlighted a mean value of 9,43 ± 5,0 mm. Moreover, the distribution of the mean error (Figure 4.9) shows a right-skewed asymmetry, with most permanent sample plots (SPP) recording values below 10 mm, but also a limited number of plots with mean errors exceeding 20 mm. Overall, 69.8% of the SPPs recorded mean errors below 10 mm, while 94.3% fell below the 20 mm threshold, which may be considered acceptable for determining individual tree dendrometric characteristics.

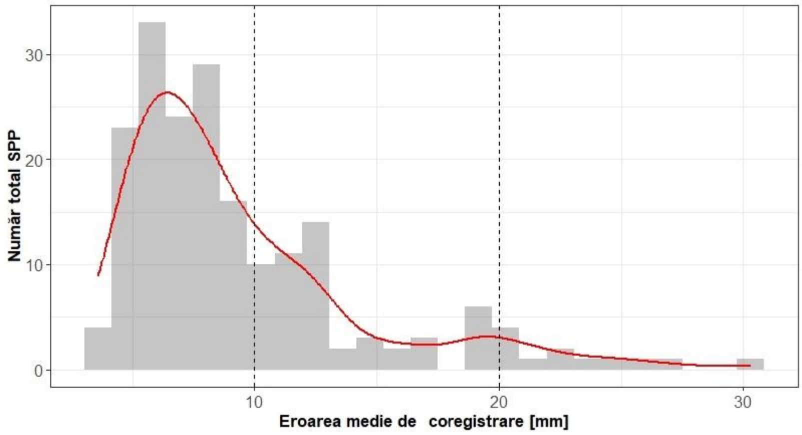

Figure 4.9 *– Distribution of the mean coregistration error (absolute values) at permanent sample plot (SPP) level.*

The analysis performed at the level of each investigated network highlights statistically significant differences in mean coregistration error (Kruskal–Wallis, $\chi^2 = 41.05$, $p < 0.001$). Thus, the FA network presented the lowest values (7.14 ± 3.3 mm), with 90.8% of the SPPs having a mean coregistration error below 10 mm and 97.4% below 20 mm. In comparison, the AM network recorded a mean coregistration error of 10.9 ± 5.5 mm, while the MO network recorded a mean coregistration error of 11.2 ± 4.6 mm. The comparative analysis of the mean coregistration error among the networks, performed using the Wilcoxon test (with p-value adjustment through the Benjamini–Hochberg method), confirms significant differences between the FA network and the other two networks ($p < 0.001$), whereas no significant differences were identified between the AM and MO networks ($p = 0.35$).

In addition, a total of 11 permanent sample plots (SPP) recorded mean coregistration errors ≥ 20 mm, distributed across all inventory networks: 7 SPPs in the AM network and two SPPs in each of the FA and MO networks. The analysis of the relationship between the minimum overlap percentage and the mean coregistration error highlighted that some of these cases were associated with reduced overlap between point clouds, also indicating an influence of scan geometry conditions on the stability of the coregistration process.

Overall, although variations among the inventory networks and isolated cases with mean coregistration errors exceeding 20 mm were observed, the multiple scan coregistration process may be considered robust, as the majority of the permanent sample plots (94.3%) fall within limits compatible with the analysis of tree-level dendrometric characteristics.

A low level of coregistration errors was also observed, indicating an adequate spatial alignment of the scans and thereby allowing subsequent analyses at individual tree level, without geometric deviations significantly affecting the identification and localization of tree stems. In this context, the point clouds were subjected to a segmentation process, through which the raw data structure was decomposed into distinct sets of points associated with individual trees (clusters), allowing the separate identification and analysis of each tree (Figure 4.10).

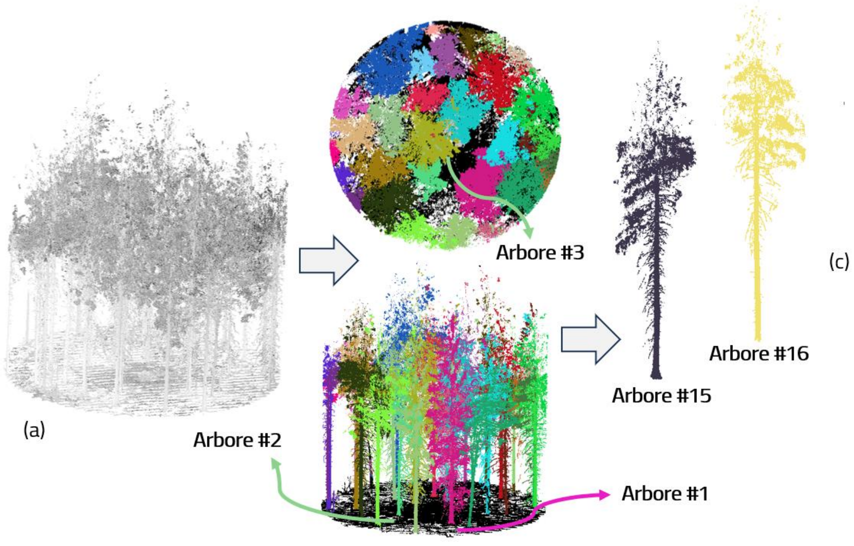

Figure 4.10 *– Three-dimensional point cloud obtained through the coregistration of different scan positions, permanent sample plot (SPP) 232 (a); segmented point cloud, where each tree is assigned a position and a unique identification number (ID) (b); segmented trees resulting from the point cloud (c).*

In order to evaluate the performance of individual tree detection, a spatial matching procedure was carried out between the trees resulting from the individual segmentation process and the trees inventoried in the field, at the level of each permanent sample plot (SPP). The association was performed based on spatial proximity, by assigning each detected stem to the nearest reference tree. The association was validated only in cases where the planimetric distance between the position of the TLS-identified tree and the position of the inventoried tree was less than 1 m; otherwise, the association was rejected.

Based on the correspondence established between the trees obtained through the TLS method and the trees inventoried in the field, a confusion matrix was constructed by assigning each tree to one of the following categories: TP – correctly detected trees (matching trees), FN – reference trees that were not detected, and FP – trees segmented from the point clouds that do not correspond to any reference tree. This classification allowed the quantification of detection performance at permanent sample plot (SPP) level.

By aggregating the results obtained for all three inventory networks, a total number of 6927 reference trees was obtained, of which 6562 (94.7%) were correctly detected (TP), 365 (5.3%) trees were not detected (FN), while 713 trees were segmented from the point clouds without corresponding to any reference tree. Thus, a detection accuracy of 0.947 and a precision of 0.902 were obtained (F1-score = 0.924).

The analysis at permanent sample plot (SPP) level indicates a high detection accuracy (0.954), with most permanent sample plots recording values above 0.90 in terms of detection performance. Even in the least favorable cases, the detection accuracy value does not fall below 0.730 (Figure 4.11). Detection precision records a mean value of 0.908, while the F1-score reaches a mean value of 0.930, confirming a balance between correctly detected trees (TP) and trees without correspondence.

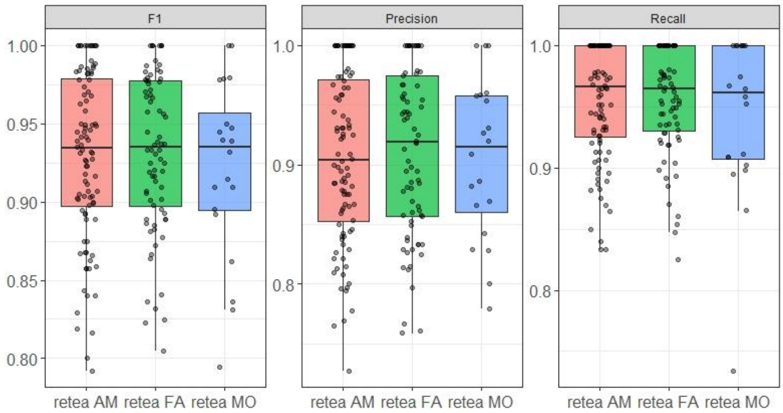

***Figure 4.11** – Graphical representation of the variability of F1-score, detection precision, and detection accuracy in relation to the permanent sample plot (SPP).*

The analysis of the relationship between the total number of trees inventoried within the permanent sample plots (SPP) and detection accuracy highlights a statistically significant negative association (Spearman's rho coefficient = -0.312, $p < 0.001$). The obtained results indicate a tendency for detection performance to decrease in plots containing a higher number of trees. This relationship suggests that stand density and structural complexity may influence the segmentation process by increasing the frequency of omissions (FN) in denser plots.

The relationship between the number of inventoried trees (N) within the permanent sample plots (SPP) and the number of correctly detected trees (TP) indicates a very strong association (Pearson correlation coefficient r = 0.985; $p < 0.001$), highlighting a direct proportionality between the number of existing trees and those identified through segmentation. At the same time, the analysis of the relationship between the number of inventoried trees (N) and detection accuracy revealed a statistically significant negative association (Spearman's rho coefficient = -0.312; $p < 0.001$), indicating a tendency for detection accuracy to decrease in plots containing a large number of trees (Figure 4.12).

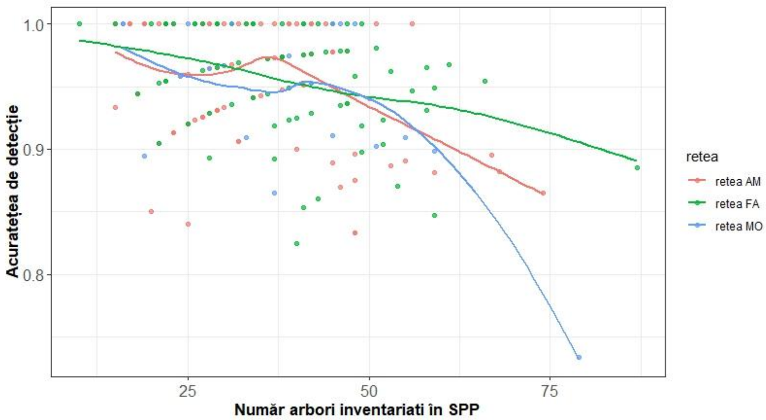

***Figure 4.12** – Relationship between detection accuracy and the number of inventoried trees*

In order to evaluate the accuracy of dendrometric parameters derived from TLS, the diameter at breast height (dbh) and tree height values obtained through segmentation were compared, at individual tree level, with the reference values obtained through field-based forest inventories, for the correctly identified (matching) trees.

The dendrometric characteristics of trees were extracted from the point clouds resulting from the segmentation of individual trees using the algorithms implemented in the *ITSMe* package (Terryn et al. 2023). Following processing, the main structural variables were estimated, namely diameter at breast height (dbh), total tree height (h), and crown projection area (CPA). These variables were automatically derived for each tree identified within the point clouds and were used for the dimensional characterization of the analyzed trees.

Tree crown diameter (CD) was calculated based on the horizontally projected area of the point cloud corresponding to the crown ($CD = 2 \cdot \sqrt{CPA/\pi}$), using its convex representation. Height to crown base (HCB) was determined through the classification of crown points and stem points, resulting as the lowest height of the points classified as crown. Crown length (CL) was calculated as the difference between total tree height and height to crown base (CL = h − HCB). Crown asymmetry (asim) was determined as the ratio between crown projection area and the area of the circle formed by the maximum crown radius (R_{max}) of the tree crown (Figure 4.13).

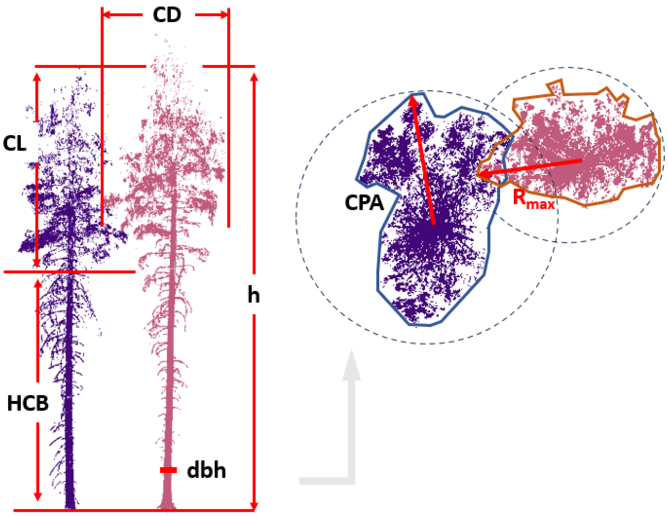

Figure 4.13 *– Estimation of tree dendrometric characteristics extracted from segmented point clouds: crown diameter (CD); crown length (CL); height to crown base (HCB); diameter at breast height (dbh); total tree height (h); crown projection area (CPA); maximum crown radius (R_{max}).*

The analysis of the obtained results highlighted that the estimation of diameter at breast height (dbh) through terrestrial laser scanning (TLS) produced dbh estimates very close to the values of the reference trees. The values of the coefficient of determination (R^2) ranged between 0.967 (MO network) and 0.978 (FA network), indicating a very strong linear relationship between the TLS-derived values and the reference values.

Considering all three analyzed networks, the degree of agreement between the diameter values estimated through terrestrial laser scanning and the diameter values of the reference trees was evaluated using Lin's Concordance Correlation Coefficient (CCC)) (Bornand et al. 2023). The obtained values highlight estimates that are very close to the values of the reference trees (Table 4.10). In the AM network, the CCC coefficient was 0.987 for beech and 0.988 for spruce. In the FA network, the CCC value was 0.989 for beech, while in the MO network the CCC value was 0.983, indicating that the dbh values estimated through terrestrial laser scanning are very close to those measured in the field for the reference trees.

The tendency to deviate from the mean value (Bias) was low and positive across all analyzed networks, indicating a slight systematic overestimation of diameter at breast height in the values derived from TLS data. Bias values ranged from 0.25 cm (AM network, spruce species) to 0.36 cm (AM network, beech species), resulting in an average deviation of less than 0.4 cm compared to the reference values (Table 4.6).

The root mean square error (RMSE) ranged between 1.74 cm (FA network, beech species) and 2.35 cm (MO network, spruce species), while the mean absolute error (MAE) varied between 1.35 cm and 1.87 cm. In addition, the relative root mean square error (RRMSE) ranged from 6.03% to 7.38%, indicating low variability in the dbh estimates obtained through TLS point cloud processing.

Table 4.6 *– Accuracy indicators for diameter at breast height*

Inventory network	Species	Bias [cm]	RMSE [cm]	MAE [cm]	RRMSE [%]	R^2	r	CCC
network AM	beech	0,36	1,90	1,47	7,38	0,974	0,986	0,987
	spruce	0,25	2,05	1,60	6,03	0,977	0,988	0,988
network FA	beech	0,26	1,74	1,35	6,28	0,978	0,988	0,989
network MO	spruce	0,27	2,35	1,87	6,46	0,967	0,983	0,983

The results obtained from total tree height estimation showed higher variability and a relatively systematic tendency to underestimate tree height. However, the coefficient of determination (R^2) ranged between 0.565 (FA network) and 0.784 (AM network, spruce species), indicating a moderate relationship between the TLS-derived values and the reference measurements.

Considering all three analyzed networks, the tendency to deviate from the mean value (Bias) was negative, with values ranging between –1.76 m (AM network, beech species) and –2.65 m (FA network), indicating a systematic underestimation of tree heights derived from terrestrial laser scanning. The root mean square error (RMSE) ranged between 4.31 m and 5.24 m, while the mean absolute error (MAE) varied between 3.35 m and 4.28 m. In relative terms, the RRMSE ranged from 16.9% to 23.8% (Table 4.7), values significantly higher than those obtained for dbh.

Considering all three analyzed networks, the level of agreement between tree height values estimated through terrestrial laser scanning and those measured in the field for the reference trees was high in all cases (Table 4.7). The CCC values ranged between 0.712 and 0.829, indicating good to very good agreement between the two datasets. The highest values were recorded in the AM network (0.829 for beech species and 0.858 for spruce species), followed by the MO network (0.817), while a lower value was obtained for the FA network (0.712).

Table 4.7 *– Accuracy indicators for the height of trees segmented from terrestrial laser scanning data*

Inventory network	Species	Bias [m]	RMSE [m]	MAE [m]	RRMSE [%]	R^2	r	CCC
network AM	beech	-1,76	4,37	3,35	18,3	0,707	0,841	0,829
	spruce	-2,20	4,54	3,61	16,9	0,719	0,885	0,858
network FA	beech	-2,65	5,64	4,28	23,8	0,565	0,752	0,712
network MO	spruce	-2,51	4,57	3,49	18,3	0,784	0,848	0,817

Tree height estimates obtained through terrestrial laser scanning (TLS) were generally characterized by a tendency toward underestimation across all investigated networks. This tendency was less pronounced in the AM network and more evident in the FA network, while in the MO network it remained relatively consistent. However, the deviation from the reference values was not uniform across the entire range of tree height variation.

In the AM network, for beech species, the error was minimal within the 35–40 m range, while above this interval a slight overestimation was observed. In contrast, for spruce species, the estimates were underestimated throughout the entire analyzed range (Figure 4.23). Regarding the FA network, tree heights estimated through TLS were underestimated up to approximately 33 m, after which an overestimation trend emerged. Conversely, in the MO network (spruce species), TLS estimates showed a consistent underestimation without a reversal of the trend.

The overestimation observed for beech species may be associated with the difficulty of identifying the actual tree top in irregular crowns. Under such conditions, the local maximum point within the point cloud may correspond to a lateral branch or to segmentation errors, leading to slightly overestimated height values. In contrast, for spruce, where the apex is well defined and clearly positioned above the crown, such situations (overestimation) are less frequent, and the estimates are predominantly characterized by underestimation. This behavior reflects a specific limitation of TLS technology, which scans trees laterally and from the base toward the top, thereby reducing the probability of fully capturing the upper part of the crown.

To assess the statistical significance of the observed differences between the inventory networks, the distribution of absolute height errors was analyzed using the Kruskal–Wallis test. The obtained results revealed statistically significant differences between groups ($\chi^2 = 62.50$; df = 3; $p < 0.001$). Absolute height error varied among the networks, with higher median values recorded in the FA network, the difference being statistically significant ($p < 0.001$) (Figure 4.14).

Regarding the tendency to deviate from the mean value (Bias), all networks exhibited a systematic underestimation of tree height, reflected by negative residual values (Table 4.7), ranging between –1.76 m and –2.65 m, indicating that TLS estimates consistently underestimated the reference values.

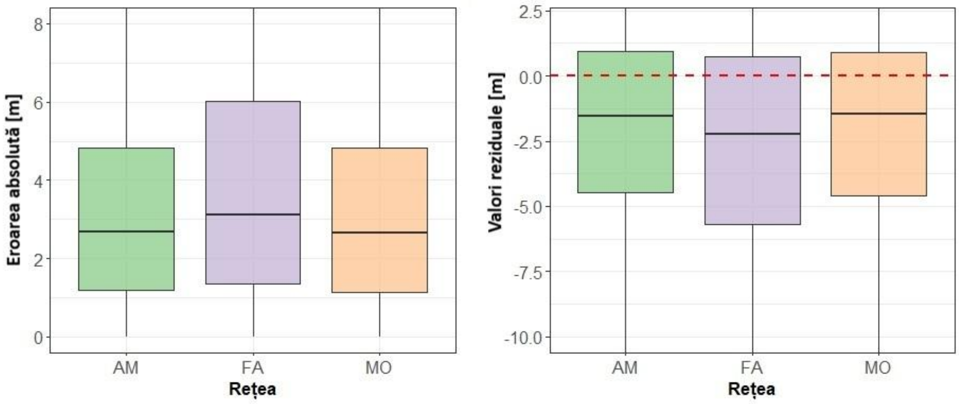

(a) (b)

***Figure 4.14** – Distribution of tree height estimation errors: absolute error (a) and residual values (b).*

The systematic underestimation of the estimated tree heights can be explained by inherent technological limitations and by the structural complexity of the analyzed stands. In the case of terrestrial laser scanning (TLS), detection of tree tops is frequently affected by occlusion effects generated by neighboring trees, canopy stratification, and the irregular geometry of tree crowns.

It should also be noted that, in dense or multi-layered stands, the laser beam is not always able to intercept the tree apex, particularly when it is partially obscured by lateral branches or vertically overlapping trees. This situation leads to an incomplete reconstruction of the upper third of the crown and, consequently, to underestimated total tree height values.

The higher RMSE and RRMSE values recorded in the FA network (RMSE = 5.64 m; RRMSE = 23.8%) suggest a stronger influence of stand structure on estimation performance compared to the AM network (RMSE = 4.37 m; RRMSE = 18.3%), where the errors were lower. The negative dependence of residual values on reference height confirms that the underestimation becomes more pronounced for taller trees, indicating a structural rather than random nature of the error.

To evaluate the accuracy of tree height estimation derived from the co-registration of point clouds obtained from terrestrial laser scanning and UAV data, individual tree height values were compared with reference values obtained through field-based forest inventories for the corresponding correctly identified trees.

The analysis of Pearson correlation coefficients (r) revealed a strong relationship between tree heights estimated from remote sensing data and the reference tree values. The (r) values were high across all analyzed networks, ranging from 0.921 (MO network) to 0.938 (AM network), confirming a very strong linear association between the two datasets. The coefficient of determination (R^2) supports this trend, indicating that approximately 85% of the variation in the reference heights is explained by the estimated values (Table 4.8).

In addition, the concordance correlation coefficient (CCC) showed values ranging between 0.862 and 0.903, indicating estimates very close to the reference tree values (Table 4.8). Regarding estimation accuracy, the root mean square error (RMSE) varied between 2.79 m and 2.96 m, while the mean absolute error (MAE) ranged from 2.23 m to 2.36 m. The Bias values were low, ranging between –0.33 m and 0.98 m, indicating the absence of a significant systematic tendency toward overestimation or underestimation of tree heights.

Table 4.8 *– Accuracy indicators for tree height derived from the co-registration of point clouds obtained from terrestrial laser scanning (TLS) and UAV data*

Inventory network	Species	Bias [m]	RMSE [m]	MAE [m]	RRMSE [%]	R^2	r	CCC
network AM	beech	0,98	2,94	2,36	12,3	0,857	0,925	0,893
	spruce	-0,07	2,96	2,36	11,9	0,881	0,938	0,903
network FA	beech	0,96	2,87	2,27	12,1	0,856	0,925	0,865
network MO	spruce	-0,33	2,79	2,23	10,4	0,849	0,921	0,862

Tree height estimates obtained through the integration of TLS and UAV data were generally characterized by a high level of agreement with the reference tree height values across all analyzed networks (Figure 4.25). Compared to estimates based exclusively on terrestrial laser scanning (TLS), the differences were smaller and the general tendency toward underestimation was substantially reduced, without evidence of a clear systematic bias.

However, the deviation from the reference values was not constant across the entire range of tree height variation. In the AM network, the estimated values were close to the reference values. Thus, for beech species, both in the AM and FA networks, a slight tendency toward overestimation was observed, more evident for large trees (over 25 m). For spruce species, the estimated values remained close to the reference values, without a clear tendency toward underestimation or overestimation.

These results indicate that the integration of TLS and UAV data improves tree height estimation by compensating for limitations specific to TLS technology. UAV data capture the upper third of tree crowns more effectively, allowing a more accurate identification of tree tops. By complementing information from the upper crown area and reducing the occlusion effect, the specific differences observed in estimates based exclusively on TLS scans are reduced, and the agreement between estimated and reference values becomes higher across the entire range of tree height variation.

To evaluate the statistical significance of the differences between the inventory networks, the distribution of absolute height errors was analyzed using the Kruskal–Wallis test. The obtained results did not indicate statistically significant differences between groups (χ^2 = 0.802; df = 3; p = 0.848). Absolute height error was similar among the networks, with median values around 2.4 m. The FA network showed slightly higher variability, although the differences were not statistically supported (Figure 4.15).

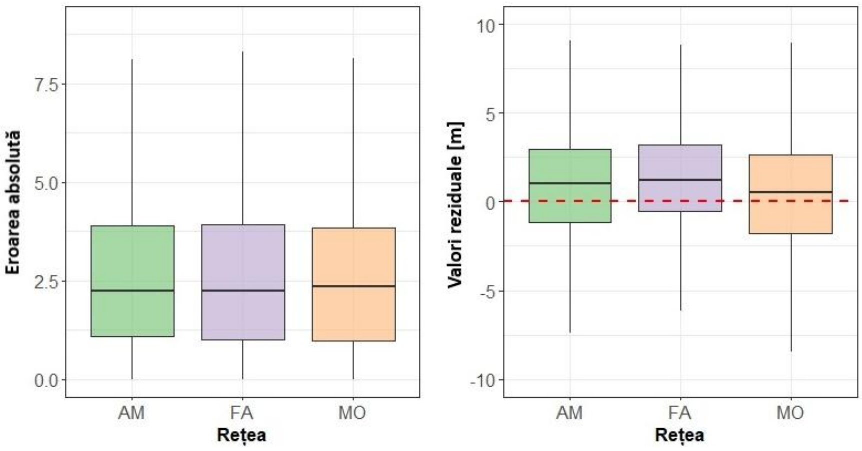

Figure 4.15 *- Distribution of tree height estimation errors obtained from the co-registration of TLS and UAV point clouds.*

The assessment of competition intensity at the individual tree level was performed using the algorithms implemented in the *TreeCompR* package (Rieder et al. 2024). The analysis of Pearson correlation coefficients (r) revealed negative relationships between the calculated competition indices and the main dendrometric characteristics of trees, including diameter at breast height, tree height, and crown projection area (Figure 4.16).

The obtained results indicate that the competition index CI_RK3 (Rieder et al. 2024) has a significant negative effect ($p < 0.001$) on tree dendrometric characteristics. Trees subjected to intense competition exhibited lower values of diameter at breast height (dbh) and height (h), as well as more limited crown development. The identified correlations were more pronounced for dbh ($r = -0.655$, $p < 0.001$) and h ($r = -0.686$, $p < 0.001$) compared to crown projection area ($r = -0.304$, $p < 0.001$). In the case of radial growth, the correlation with CI_RK3 was moderate ($r = -0.466$, $p < 0.001$), indicating a reduction in growth rate under conditions of high competition (Figure 4.17).

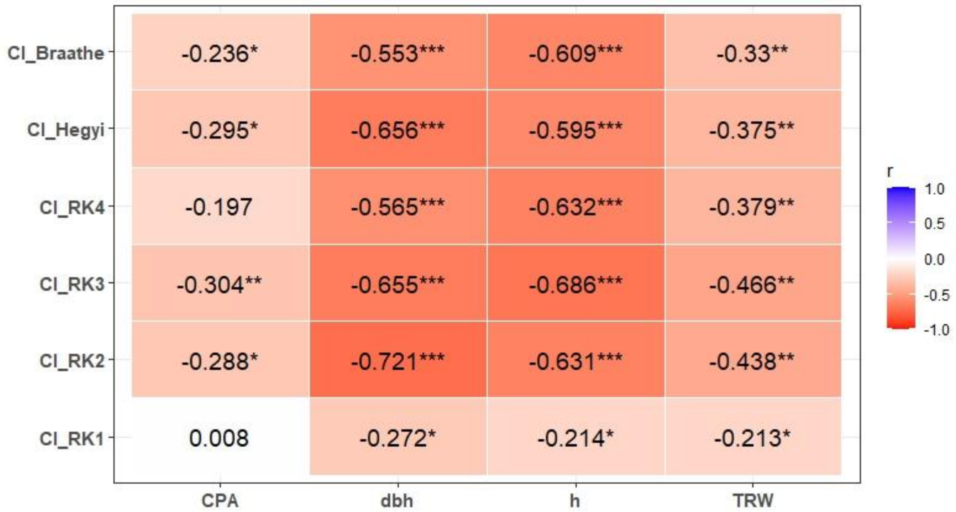

Figure 4.16 - *Matrix of Pearson correlation coefficients (r) between competition indices and the main dendrometric characteristics of trees*

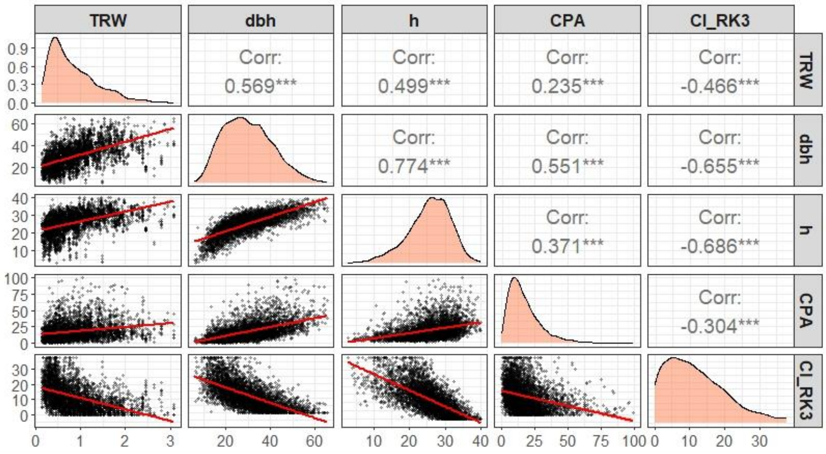

Figure 4.17 – *Matrix of Pearson correlation coefficients (r) between the RK3 competition index and the main dendrometric characteristics of trees*

4.3. ANALYSIS OF RADIAL GROWTH INCREMENT CORE SAMPLES

Following the collection of radial growth samples, a total of 1,180 valid individual samples were obtained from 96 permanent sample plots distributed across the three statistical inventory networks (AM network, FA network, and MO network). In the AM network (48 permanent sample plots), radial growth samples were collected from 667 trees, of which 356 belonged to spruce species and 311 to beech species. In the FA network (38 permanent sample plots), a total of 405 growth samples were collected, while in the MO network (10 permanent sample plots), 108 samples were obtained. Therefore, at the level of the entire dataset, 716 increment cores were collected for beech species, representing 60.6% of the total number, while 464 cores (39.4%) were collected for spruce species.

To analyze differences in species distributions of the number of increment cores collected across diameter at breast height classes (2 cm intervals) between the inventory networks, the Kolmogorov–Smirnov (KS) significance test was applied. For beech species, no significant differences were identified between the FA and AM networks ($D = 0.040$; $p = 0.942$). Similarly, for spruce species, the comparison between the MO and AM networks did not reveal statistically significant differences ($D = 0.379$; $p < 0.001$). In contrast, within the AM network, statistically significant differences were identified between beech and spruce species ($D = 0.379$; $p < 0.001$) (Figure 4.18).

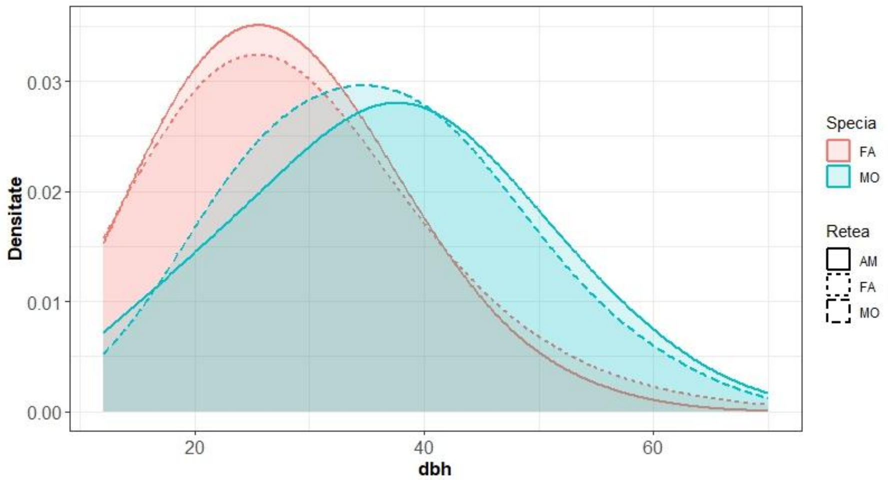

Figure 4.18 – *Distribution of increment cores by diameter at breast height classes (2 cm), according to the statistical inventory network and species.*

Within the statistical inventory networks, the mean radial growth over the last 10 years (2015–2024) showed variable values depending on species and network. In the AM network, beech exhibited a mean annual growth of 0.83 $mm*year^{-1}$, while spruce recorded 0.99 $mm*year^{-1}$. Comparing the same species between networks, the differences were smaller than the interspecific variation. In the FA network, the mean annual growth was 0.70 $mm*year^{-1}$, corresponding to an approximately 15% reduction compared to beech in the AM network. The nonparametric Wilcoxon test indicated statistically significant differences between the two networks for beech species ($W=69296$; $p < 0.001$), confirming the existence of a network effect (mixed population effect) on the mean radial growth level.

For spruce species, the mean annual growth was 0.99 $mm*year^{-1}$ in the AM network and 1.10 $mm*year^{-1}$ in the MO network, representing approximately 14% higher growth in the MO network compared to the AM network. In this case, the nonparametric Wilcoxon test did not reveal statistically significant differences between the two networks ($W=16100$; $p = 0.080$). The application of the ANOVA test highlighted the existence of statistically significant differences ($F=78.83$; $p < 0.001$) between the mean radial growth values recorded for the two analyzed species (beech and spruce) across the three research networks.

4.4. MODELING TREE RADIAL GROWTH IN RELATION TO CROWN DIMENSIONS AND TREE COMPETITION

The comparative analysis of tree crown dimensional characteristics (diameter and length) and radial growth indicators, in relation to the statistical inventory networks (AM, FA, and MO networks), revealed the existence of statistically significant differences between networks, both for radial growth and crown characteristics ($p < 0.05$). Regarding radial growth indicators, the coefficient of variation of tree-ring width (cvTRW) showed significant differences among networks ($p = 0.021$), highlighting the presence of network-specific variations in tree growth patterns. In addition, the mean tree-ring width (TRW) differed significantly among the statistical inventory networks ($p = 0.012$).

At the same time, significant differences were also identified for crown characteristics. The asymmetry index (asim), crown projection area (CPA), crown radius (CR), and the ratio between crown length and crown radius (CSLC) showed significant variation among the statistical inventory networks ($p < 0.001$), indicating that, at the individual tree level, trees from the three inventory networks were characterized by different crown shapes, reflecting distinct competition conditions and vertical structural organization of the forest stands.

Pearson correlation analysis revealed the existence of moderate correlations between growth indicators and crown characteristics. Radial growth (TRW) was positively correlated with crown length (CL; $r = 0.460$), tree height (h; $r = 0.480$), and crown diameter (CD; $r = 0.250$), and negatively correlated with competition indices (CI; $r = -0.330$) (Figure 4.19). In addition, basal area increment (BAI) showed moderate to strong positive correlations with crown dimensions, especially crown length (CL; $r = 0.570$), but also with tree height ($r = 0.590$), as well as a moderate negative correlation with competition indices (CI; $r = -0.400$).

The coefficient of variation of radial growth (cvTRW) showed weak to moderate correlations with crown dimensions, presenting negative correlations with crown length (r = –0.110) and tree height (r = –0.120), as well as weak positive correlations with competition indices (r = 0.070). *These results suggest that trees with more developed crowns tend to exhibit more stable radial growth, while competition is associated with slightly higher variability in radial growth.*

Overall, it can be highlighted that crown variables, particularly crown length (CL), are positively associated with TRW, whereas the competition index (CI) has a moderate negative effect. Pearson correlation coefficient (r) values ranging between 0.3 and 0.6 reflect moderate to strong linear associations between crown variables and radial growth indicators. These results indicate that a significant proportion of radial growth variation is associated with crown dimensions.

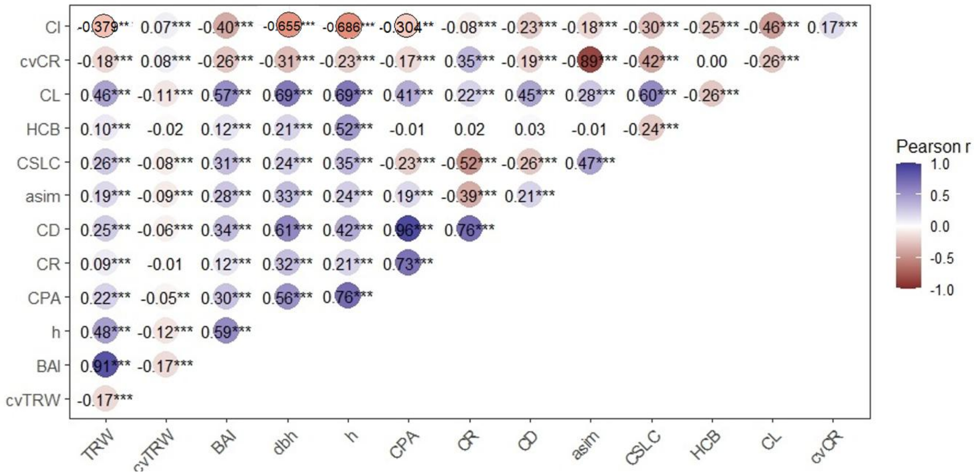

Figure 4.19 *– Correlation between crown variables and growth indicators: radial growth – TRW; coefficient of variation of radial growth – cvTRW; basal area increment – BAI; diameter at breast height – dbh; tree height – h; crown projection area – CPA; crown radius – CR; crown diameter – CD; crown asymmetry – asim; ratio between crown length (CL) and crown radius (CR) – CSLC; height to crown base – HCB; coefficient of variation of crown radius – cvCR.*

To evaluate, at the level of each inventory network (AM, FA, MO), the interaction between crown characteristics and radial growth, linear mixed models were applied, taking into account the hierarchical structure of the data at the permanent sample plot (SP) level.

The obtained results highlighted that crown length (CL) has a positive and significant effect ($p < 0.001$) on radial growth. Across all analyzed stand types, trees with longer crowns exhibited, on average, higher radial growth values. Although the strength of the relationship varied among the networks, its direction remained consistently (positive).

A comparative analysis revealed that the linear relationship between crown length (CL) and radial growth was significantly stronger in mixed stands (AM network) than in beech stands (FA network; β = 0.0138; $p < 0.001$). The differences recorded between the regression lines specific to the AM and MO networks were at the limit of statistical significance ($p = 0.055$), while no significant differences were identified between those corresponding to the FA and MO networks ($p = 0.925$). Thus, stand type was found to influence the strength of the relationship between crown length (CL) and radial growth, without altering its direction.

A similar pattern was observed for crown diameter (CD), which also had a positive and statistically significant effect ($p < 0.001$) on radial growth. Therefore, crown dimensions, expressed through CL and CD, were positively associated with radial growth, and this relationship was present across all statistical inventory networks, with moderate differences in intensity among them.

Regarding the explanatory capacity of the adopted models, the model including the interaction CL × network (AM, FA, MO) explained 26.4% of the variation in radial growth (R^2= 0.264), and 37.1% when variation among sample plots within each network was also included (R^2= 0.371). The model including CD explained 20.6% of the variation in radial growth (R^2= 0.206), and 36.0% when variation among permanent sample plots (SP) was additionally considered (R^2= 0.360). Thus, crown length (CL) showed higher explanatory power, while crown diameter (CD) had larger coefficients, suggesting a stronger sensitivity of radial growth to variation in crown width.

To evaluate the simultaneous contribution of CL and CD to radial growth (TRW), a linear mixed model of the following form (3) was applied:

$$TRW_i \sim CL * rețea + CD * rețea + (1|SP) \qquad (3)$$

where:
TRW_i represents tree-ring width, mm;
CL - crown length, m;
CD - crown diameter, m;
network – statistical inventory network (AM, FA, MO);
SP - permanent sample plot.

The obtained results showed that the model simultaneously including crown length (CL), crown diameter (CD), and their interactions with stand type (AM, FA, MO networks) revealed positive effects of both variables on radial growth (Figure 4.20). The estimated coefficient (β) for CL was 0.044 ($p < 0.001$), while for CD it was 0.057 ($p < 0.001$), indicating that each of the two crown dimensions independently contributes to explaining TRW variation. The interaction terms showed that the effect of CL varies among networks, whereas the effect of CD is more stable across the statistical inventory networks.

The comparison of candidate models based on the AIC criterion showed that the model including both CL and CD described the data considerably better than the model including CL as the sole variable (ΔAIC = 123), indicating that CD improves the model and contributes positively to explaining radial growth. The model explained 28.7% of the variation in radial growth (R^2 = 0.287) and approximately 40% when variation among sample plots was also considered (R^2 = 0.404). Furthermore, the variance inflation factor values for the explanatory variables (crown length and crown diameter) (VIF < 2.1) satisfied the collinearity condition, supporting the stability of the obtained estimates and justifying their simultaneous use in the model.

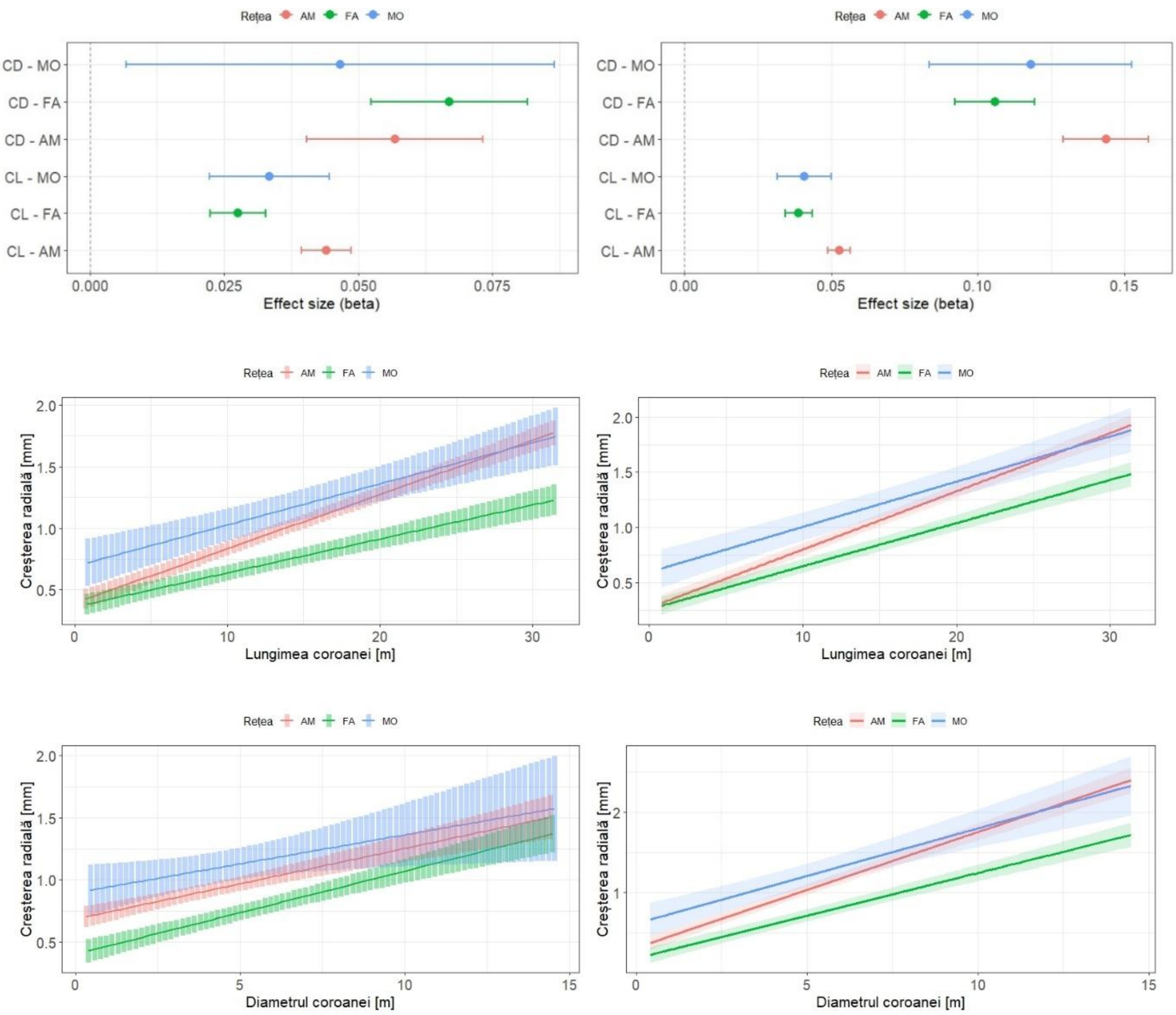

Figure 4.20 *– Impact of stand types on the relationship between radial growth and the crown variables CL/CD. The graphs on the left illustrate the estimated relationships based on the combined model simultaneously including crown length (CL) and crown diameter (CD).*

To quantify the effect of local competition on radial growth, a linear mixed model (4) was applied, including the standardized crown variables previously used (CLz, CDz), as well as the standardized value of the competition index (CIz). Prior to modeling, the variables were scaled to the 0–1 interval using the min–max transformation $f(x) = (x_i - x_{min}) / (x_{max}-x_{min})$, where represents the estimated value of the variable, and x_{min} and x_{max} represent its minimum and maximum values, respectively. The model included interactions between the explanatory variables and the statistical inventory networks, as well as a random intercept at the permanent sample plot (SP) level.

$$TRWz_i \sim CLz * rețea + CDz * rețea + CIz + CLz:CIz + CDz:CIz + (1|SP) \qquad (4)$$

where:

$TRWz_i$ represents the standardized value of annual ring width, mm;

CLz - standardized value of crown length, m;

CDz – standardized value of crown diameter, m;
network – statistical inventory network (AM, FA, MO);
CIz - standardized value of the competition index, m;
SP - permanent sample plot.

The analyses revealed that the competition index (CIz) had a strong and significant negative effect on the standardized radial growth values (TRWz) ($\beta = -0.194$, SE = 0.022, t = –8.97, $p < 0.001$), indicating a reduction in radial growth with increasing local competition intensity. Crown length (CLz) showed the strongest positive effect on TRWz ($\beta = 0.329$, $p < 0.001$), while crown diameter (CDz) also had a significant positive effect ($\beta = 0.159$, $p < 0.001$), highlighting that trees with more developed crowns exhibit higher radial growth values (Table 4.9).

The interaction between crown length and competition (CLz : CIz) was negative and significant ($\beta = -0.110$, $p < 0.001$), indicating that the favorable effect of a long crown is reduced under conditions of high competition. In contrast, the interaction between crown diameter and competition (CDz : CIz) was not significant ($p = 0.920$), suggesting that the influence of crown diameter on radial growth is not conditioned by competition intensity in the same way.

The effects associated with the statistical inventory networks indicate structural differences among stand types. Compared to the AM network, the FA network recorded significantly lower TRWz values ($\beta = -0.334$, $p < 0.001$), while the MO network showed significantly higher values ($\beta = 0.317$, $p = 0.013$). The interaction CLz : FA network was negative and significant ($\beta = -0.100$, $p = 0.003$), indicating a weaker relationship between crown length and radial growth.

Table 4.9 - *Estimated coefficients of the fixed effects from the linear mixed model*

Fixed effect	Estimated coefficient [β]	Standard error	t-statistic	p-value
(Intercept)	0,021	0,052	0,412	p = 0,681
CLz	0,329	0,023	13,738	p < 0,001
networkFA	-0,334	0,078	-4,260	p < 0,001
networkMO	0,317	0,125	2,519	p = 0,013
CDz	0,159	0,025	6,125	p < 0,001
CIz	-0,194	0,021	-8,967	p < 0,001
CLz: networkFA	-0,099	0,034	-2,923	p = 0,003
CLz: networkMO	-0,109	0,057	-1,913	p = 0,056
networkFA:CDz	0,024	0,034	0,693	p = 0,488
networkMO:CDz	-0,019	0,067	-0,292	p = 0,770
CLz:CIz	-0,109	0,016	-6,614	p < 0,001
CDz:CIz	-0,001	0,017	-0,099	p = 0,920

To quantify how local competition modifies the relationship between crown parameters and radial growth, the standardized values of the competition index (CIz) were summarized into three different levels using the p10, p50, and p90 percentiles. To verify the structural relevance of these thresholds, the distribution of trees according to sociological position (Kraft class) was analyzed in relation to the standardized competition index (CIz).

The χ^2 test revealed a strong and significant association between CIz and sociological position (χ^2 = 1019.4; df = 9; $p < 0.001$). Under low competition conditions, trees predominantly belonged to the upper classes (Kraft I–II), whereas under high competition conditions, Kraft classes III–V predominated. The proportion of trees in Kraft class III increased from 2.5% under low competition to more than 46% under high competition, highlighting a coherent structural gradient between sociological position and competition intensity.

The relationship between radial growth and crown length revealed an effect dependent on competition intensity. Under low competition conditions, the strength of the relationship was higher, indicating a stronger positive response of radial growth to increasing crown length. As competition intensity increased, the strength of the relationship progressively decreased, reflecting the reduction of the positive effect of crown length under conditions of high competition. This trend results from the previously identified significant negative interaction between CLz and CIz ($\beta = -0.109$, $p < 0.001$) (Figure 4.21).

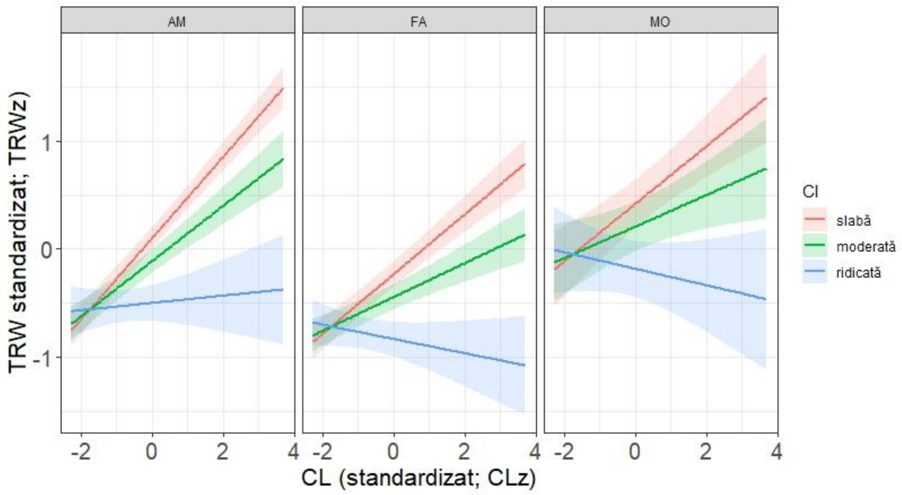

Figure 4.21 *– Effect of competition (CIz) on the relationship between crown length (CLz) and radial growth (TRWz).*

In contrast, the relationship between TRWz and CDz showed a relatively constant positive effect across competition levels, without evident changes in the strength of the relationship. The absence of a significant interaction between CDz and CIz ($\beta = -0.001$, $p = 0.920$) confirms that the influence of crown diameter (CD) on radial growth is not conditioned by competition intensity in the same way as crown length (CL). Independently of these interactions, the direct effect of competition remained negative and highly significant ($\beta = -0.194$, $p < 0.001$), indicating a systematic reduction in radial growth with increasing competition intensity (Figure 4.22).

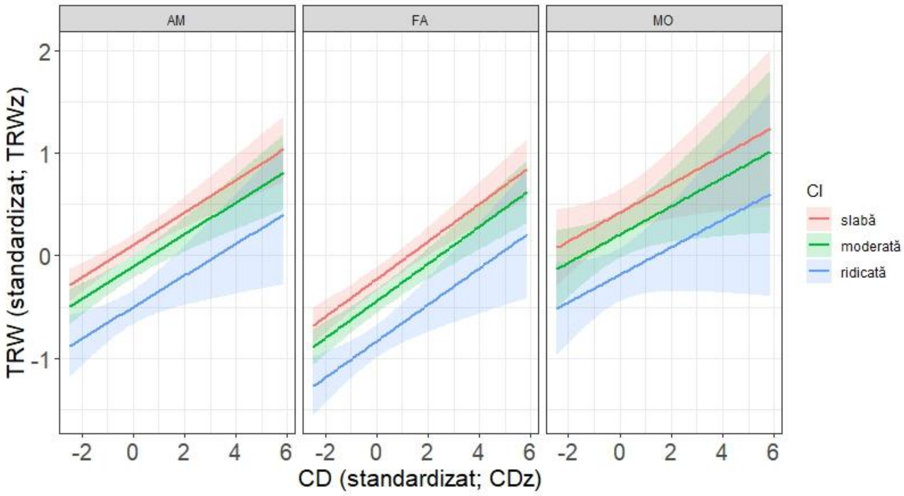

Figure 4.22 *- Effect of competition (CIz) on the relationship between crown diameter (CDz) and radial growth (TRWz).*

To evaluate the direct and indirect effects of competition on radial growth, a structural equation model (SEM) was applied and estimated at the permanent sample plot (SP) level. The structure of the fitted model included the relationships between competition (CI), crown variables (CL, CD), and radial growth. The adopted model proved to be appropriate and highly effective, showing a very good fit to the data (χ^2 = 0.066; p = 0.798; CFI = 1.00; SRMR = 0.005).

The obtained results indicate that competition intensity exerts a significant negative effect on vertical crown development (β = −0.462, p < 0.001). At the same time, CL positively influences crown diameter growth (β = 0.324, p < 0.001), highlighting the direct dependency between the two variables (Figure 4.23). The model explained 32% of the variation in crown length (R^2= 0.321) and 17% of the variation in crown diameter (R^2= 0.169).

Regarding radial growth (TRW), competition had a significant direct negative effect (β = −0.257, p < 0.001). Crown length (CL) showed a positive contribution to radial growth (β = 0.236, p < 0.029), whereas crown diameter (CD) did not have a significant direct effect on TRW (β = −0.068, p < 0.435). However, the indirect effect of competition on radial growth (TRW), mediated through CL, was significant (β_indirect = −0.109, p < 0.044). The total effect of competition on TRW was β = −0.356 (p < 0.001), indicating that approximately one-third of the influence on radial growth is exerted through crown length (CL), while the direct component remains predominant. At the permanent sample plot (SP) level, the variables included in the model accounted for 47.5% of the variation in radial growth (R^2 = 0.475) (Figure 4.23).

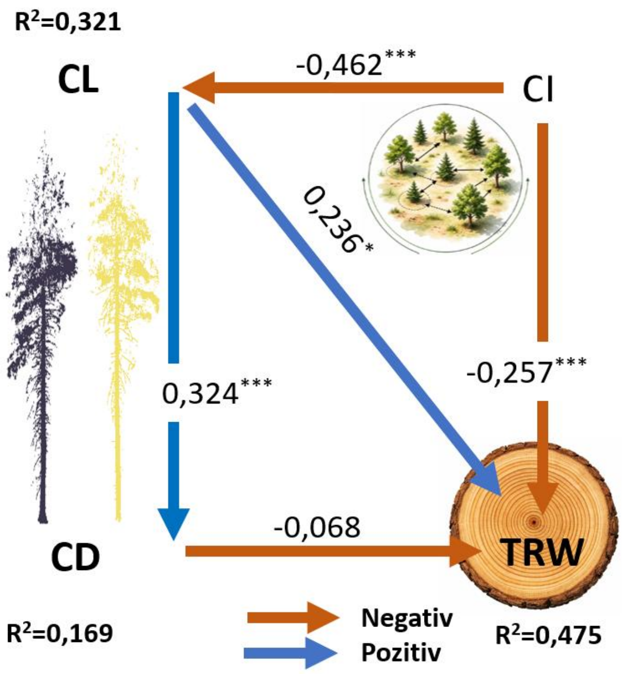

Figure 4.23 *– Graphical representation of the structural equation model (SEM).*

To evaluate the extent to which crown characteristics and competition intensity can explain the temporal dynamics of radial growth, growth curves were modeled and predicted based on tree characteristics. For this purpose, radial growth (TRW) was modeled in relation to crown dimensions, namely crown length (CL) and crown diameter (CD), as well as the competition index (CI), variables reflecting tree position within the stand and access to resources. The temporal component of radial growth was integrated by including the year of observation as an explanatory variable, together with interactions between the year of observation and the crown and competition variables, allowing the estimation of how the influence of crown characteristics and competition on radial growth changes over time.

To evaluate the direct effect of competition, two candidate models were applied. The first model considered exclusively crown variables and the temporal growth component, together with the variable defining the statistical inventory network. In the second model, the competition index (CI) and its interaction with the temporal variable were additionally included (5).

$$TRWz_i \sim CDz + CLz + CIz + year + CLz{:}year + CDz{:}year + CIz{:}year + retea + (1|tree\_id) \qquad (5)$$

where:

$TRWz_i$ represents the standardized value of annual ring width, mm;

CLz - standardized value of crown length,, m;

CDz - standardized value of crown diameter, m;

CIz - standardized value of the competition index, m;

network – statistical inventory network (AM, FA, MO);

year – year of observation;

tree_id – tree identification number.

The comparison of the two models revealed a slight improvement in performance for the model including the competition index (CI). The extended model presented a lower Akaike Information Criterion value (AIC = 10536.7) compared to the model excluding CI (AIC = 10552.3). The Likelihood Ratio Test (LRT) indicated that this difference was statistically significant (χ^2= 19.68; df = 2; $p < 0.001$). The cumulative radial growth curve, expressed using crown shape parameters, reproduced the trajectories of the measured growth values for each of the three analyzed statistical inventory networks (AM, FA, MO), with predicted values comparable to the observed ones (Figure 4.24).

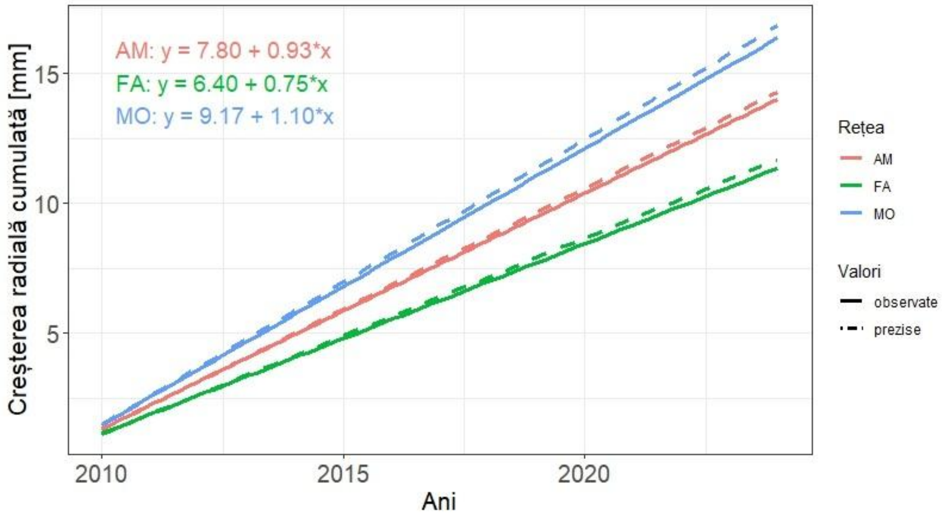

***Figure 4.24** – Observed and predicted cumulative radial growth for the three statistical inventory networks (AM, FA, MO).*

Although the inclusion of the competition index improves model performance, its contribution to explanatory capacity remains relatively low compared to crown variables. The marginal coefficient of determination (R^2_m) increased slightly from 0.169 (AM network) in the model without the competition index to R^2_m = 0.177 in the model including the competition index, while the conditional coefficient of determination (R^2_c) remained approximately constant (R^2_c = 0.686) in both cases. Similarly, the marginal coefficient of determination increased from 0.189 (FA network) and 0.215 (MO network), respectively, in the model without the competition index, to R^2_m = 0.209 (FA network) and R^2_m = 0.220 (MO network), respectively, in the model including the competition index. In contrast, the conditional coefficient of determination (R^2c) remained approximately constant, with values of R^2_c = 0.643 (FA network) and R^2_c = 0.743 (MO network) for both cases (Figure 4.25).

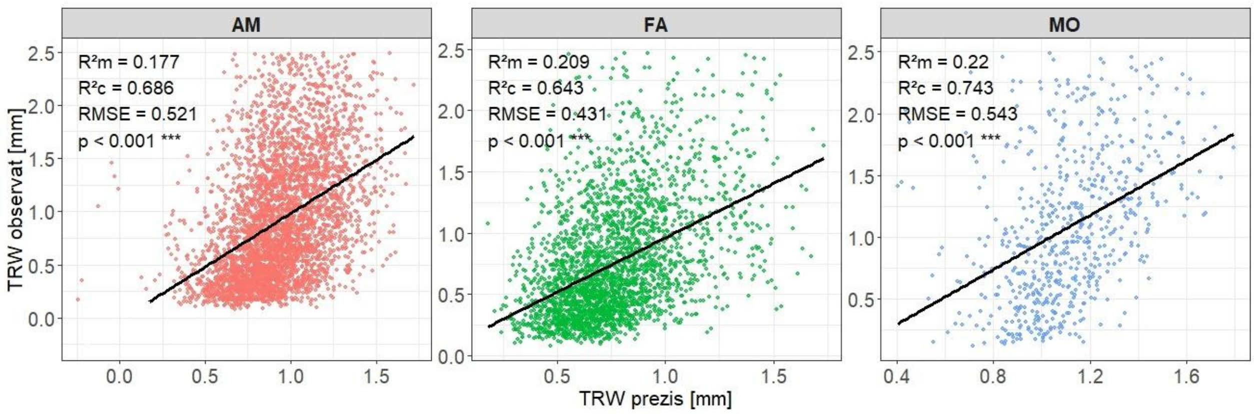

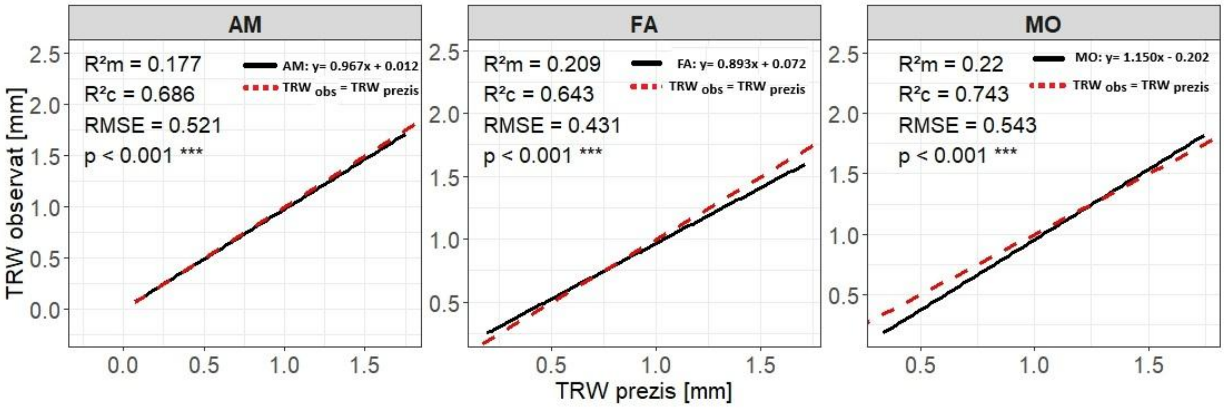

***Figure 4.25** – Relationship between observed and predicted radial growth (TRW) values estimated based on crown variables (CL; CD) for the three statistical inventory networks (AM, FA, MO).*

These results indicate that crown shape variables represent the main predictors of radial growth (TRW). The evaluation of model accuracy, performed through the comparison of measured and predicted radial growth values, indicates that crown variables can effectively estimate annual ring growth dynamics. Considering all analyzed networks, the model based exclusively on crown variables recorded an RMSE value of 0.49 mm, while the inclusion of the competition index led to a marginal reduction in error (RMSE = 0.48 mm). These findings indicate that crown variables can efficiently predict growth patterns and validate the results obtained through the application of the structural equation model (SEM).

5. CONCLUSIONS

Based on the research conducted during the doctoral thesis and the results obtained in relation to the proposed aim and objectives regarding the determination of tree dendrometric characteristics and the analysis of radial growth in forest stands from the western Southern Carpathians, using integrated remote sensing data acquired from active and passive sensors, the following conclusions can be drawn:

- **Regarding the estimation of tree dimensional characteristics through the use of remote sensing techniques.**
  - *For the estimation of tree dimensional characteristics*, the analysis of point cloud co-registration errors showed that, at the level of most permanent sample plots (SPP), point cloud co-registration was achieved within low error limits, with most values falling below the thresholds considered acceptable (below 10 mm in approximately two-thirds of the cases and below 20 mm in more than 90% of them). At the same time, the comparative analysis among the investigated research networks highlighted the best performance in trees from the beech network (FA), where most permanent sample plots (SPP) were characterized by low error ranges. In contrast, the mixed network (AM) and the spruce network (MO) showed similar values and greater variability, indicating the influence of stand structural conditions and acquisition methods on point cloud co-registration quality. Furthermore, in permanent sample plots (SPP) where higher co-registration errors (≥20 mm) were recorded, the errors were frequently associated with a low degree of overlap between scans, emphasizing the critical role of scan overlap in the stability of the co-registration process and the need to ensure appropriate remote sensing data acquisition conditions in order to obtain accurate estimates.
  - Regarding *the relationship between the number of inventoried trees and detection accuracy*, the results showed that, as the total number of trees inventoried within the permanent sample plots (SPP) increased, the number of correctly detected trees (TP) followed the same trend, reflecting the ability of the method to identify a high proportion of the reference trees (field-inventoried trees). However, detection accuracy decreased with increasing tree density within the PSPs, indicating a reduction in the efficiency of the tree segmentation process under high-density conditions. This demonstrates that, in permanent sample plots with a large number of trees, the increase in structural complexity caused by crown overlap and reduced spacing between trees leads to a higher frequency of omissions (FN), thereby affecting overall detection performance.
  - *For the estimation of tree diameter at breast height (dbh) using terrestrial laser scanning (TLS),* the results highlighted the existence of a strong agreement (very high correspondence) between the estimated values and the values measured in the field for the reference trees, characterized by very strong linear relationships and low error variability. It can therefore be stated that the use of TLS provided highly accurate estimates of the diameter at breast height measured in the field for the reference trees across all analyzed networks (AM, FA, MO), indicating high methodological stability

under different stand conditions. The high level of agreement between estimated and reference values confirms the capability of TLS technology to accurately reproduce individual tree stem dimensions. The tendency to deviate from the reference values was low and systematically positive, indicating a slight overestimation of dbh, although of small and consistent magnitude, without a significant impact on overall accuracy. This tendency highlights the presence of a minor systematic bias that does not affect the robustness or precision of the estimates. Thus, tree diameter at breast height can be determined with a high level of accuracy, confirming the strong potential of TLS for estimating tree dbh within forest stands.

- *The estimation of total tree height using terrestrial laser scanning (TLS)* is characterized by lower accuracy compared to the estimation of diameter at breast height (dbh), as well as by higher error variability. Tree height estimates are predominantly characterized by a systematic tendency toward underestimation, observed across all investigated networks (AM, FA, MO), although with varying intensity depending on the structural characteristics of the stands. This tendency is not constant across the entire tree height range, and in some situations overestimations were also observed, associated with incorrect identification of the tree top caused by specific crown characteristics.

  The systematic underestimation of tree heights is determined by the inherent limitations of TLS technology, the performance of segmentation algorithms, and stand complexity, particularly through occlusion effects generated by neighboring trees and crown stratification. Under such conditions, the laser beam does not always intercept the tree apex, resulting in an incomplete reconstruction of the upper part of the crown and, consequently, in the underestimation of total tree height. In this context, tree height estimation errors are not random in nature, but depend on stand structure and tree dimensions, indicating a systematic limitation of terrestrial laser scanning (TLS) in fully representing the upper third of tree crowns.
- *The estimation of tree height through the integration of TLS and UAV* data highlights an improvement in accuracy compared to estimates based exclusively on terrestrial laser scanning, characterized by a high level of agreement with the reference values and by reduced estimation errors. The systematic tendency toward underestimation observed in TLS-based estimates is substantially diminished, without evidence of a consistent overestimation or underestimation bias, indicating an effective correction of errors specific to terrestrial laser scanning. The improvement in performance is mainly determined by the contribution of UAV data, which enable a more complete representation of the upper part of the crown and a more accurate identification of tree tops, thereby reducing the occlusion effects characteristic of terrestrial laser scanning. Under these conditions, tree height estimates obtained through the integrated use of TLS and UAV techniques become more stable across the entire range of tree height variation, while the differences compared to the reference values measured in the field are smaller and more uniformly distributed, including in the case of large trees. At the

same time, estimation accuracy remains relatively constant among the analyzed networks (AM, FA, MO), without significant differences in error levels, indicating high applicability of the method under varying stand conditions. Thus, the integration of TLS and UAV data emerges as an effective approach for tree height estimation by compensating for TLS limitations and improving the complete representation of tree crowns.

- Regarding the *relationship between competition intensity and tree dimensional characteristics* (diameter at breast height, tree height, crown projection area), the results showed that increasing competition intensity is associated with a reduction in individual tree dimensions. Trees subjected to intense competition tended to exhibit lower values of diameter at breast height and height, as well as more limited crown development. This trend reflects the restrictions imposed by competition for essential resources such as light, water, and nutrients, leading to a reduced allocation of resources to radial growth (TRW) and overall tree development. At the same time, the identified relationships highlighted that crown dimensions play an essential role in mitigating the effects of competition, as trees with more developed crowns are able to partially reduce its negative impact. Therefore, competition intensity represents a determining factor in tree growth and development, especially under conditions of high stand density.

❖ **Regarding the determination of tree crown characteristics through remote sensing data processing and the use of radial growth models in relation to these characteristics.**

- The *estimation of tree crown characteristics* derived from remote sensing data highlighted the existence of a positive correlation between crown dimensions and tree radial growth, as well as a negative correlation between the competition index and radial growth. Thus, radial growth (TRW) was moderately positively correlated with crown length (CL) and tree height, while the correlation with crown diameter (CD) was weaker. In contrast, radial growth showed a moderate negative correlation with the competition index (CI). These findings support the hypothesis that trees with more developed crowns tend to exhibit higher radial growth values.
- The *analysis of radial growth variability* revealed the existence of weaker correlations between the coefficients of variation of radial growth (cvTRW) and crown characteristics. The coefficient of variation of radial growth was negatively correlated with crown length (CL) and tree height, and positively, although with lower intensity, correlated with the competition index (CI). These results indicate that trees with more developed crowns tend to exhibit more stable radial growth, whereas higher competition intensity is associated with slightly increased variability in radial growth (TRW) values.
- Regarding the *explanatory capacity of the applied models*, which included the interaction between crown length (CL) and radial growth across the research networks (AM, FA, MO), the results showed that CL had a greater contribution to explaining radial

growth variation compared to crown diameter (CD), particularly when variation among sample plots (SP) was also considered. At the same time, the coefficients associated with crown diameter indicated a stronger sensitivity of TRW to lateral crown variation, suggesting that the two crown dimensions (length and diameter) play complementary roles in explaining radial growth. The application of a mixed model including both crown length (CL) and crown diameter (CD), together with their interactions across the three research networks, revealed positive effects of both variables on radial growth (TRW), indicating that they contribute both independently and complementarily to explaining its variation. The inclusion of crown diameter (CD) improved model performance by approximately 12% compared to the use of crown length (CL) alone.

- Regarding the *relationship between crown variables and radial growth (TRW)* within the investigated inventory networks (AM, FA, MO), the application of the linear mixed model highlighted that crown length (CL) has a positive and significant effect on growth across all analyzed stand types (pure beech stands, pure spruce stands, and mixed spruce–beech stands). The relationship between CL and TRW was more pronounced in mixed spruce–beech stands (AM) compared to pure beech stands (FA), while for pure spruce stands (MO), the differences were small or non-significant. Tree crown diameter (CD) also exerted a positive and significant effect on radial growth (TRW), present across all analyzed networks (AM, FA, MO), with moderate variations in the strength of the relationship. The application of the structural equation model (SEM), which considered the relationships among crown characteristics, the competition index, and radial growth, demonstrated that the effect of competition on radial growth was not exclusively direct, but was partially mediated through changes in crown dimensions, particularly through the reduction of crown length (CL). Consequently, competition acted both through the direct limitation of growth and through the modification of crown dimensions, leading to a more complex overall effect on radial growth (TRW). In this context, the obtained results highlighted that crown length (CL) represents the main indicator through which competition influences radial growth, whereas crown diameter did not show a significant direct contribution.
- Regarding the *temporal modeling of radial growth (TRW) dynamics*, two candidate models were applied. The first model considered exclusively the standardized crown variables (CLz, CDz) together with the year of observation, while the second model additionally integrated the standardized competition index and its interaction with the temporal variable (year of observation). The comparison of the two models revealed an improvement in the performance of the model including the standardized competition index. Although the inclusion of the competition index improved model performance, its contribution to explanatory capacity remained relatively low compared to crown variables. At the same time, the results highlighted that crown variables derived from remote sensing data represent the main predictors of growth variation, being capable of reproducing the trends observed across the inventory networks. These findings indicate that crown dimensions estimated through remote sensing integrate the

effects of competition and reflect the level of competition among trees, constituting key variables for explaining and modeling radial growth.

- **Regarding the analysis of tree radial growth based on data obtained through remote sensing techniques in comparison with data derived from measurements collected during field inventories.**
  - The *analysis of the correlation between crown characteristics (crown length and crown diameter), the competition index, and radial growth* revealed that the influence of crown dimensions on radial growth is not uniform, but depends on competition intensity. While crown diameter exerts a relatively constant positive effect on radial growth regardless of competition intensity, crown length exhibits an effect dependent on competition intensity, with its contribution progressively decreasing under conditions of high competition. This differentiation indicates that horizontal crown development acts as a stable growth factor, whereas vertical crown development (crown length) is more sensitive to the constraints imposed by local competition. It was also found that competition intensity among trees exerts a direct negative effect on radial growth, systematically reducing growth levels as competition intensifies. At the same time, the structural equation model (SEM) highlighted that this effect is not exclusively direct, but is partially mediated through changes in crown characteristics, particularly through the reduction of crown length (CL). Thus, competition influences radial growth both through the direct limitation of space and light resources and indirectly through modifications in tree crown dimensions.
  - The analysis of *mean annual radial growth* highlighted the existence of statistically significant differences between the values recorded for the two analyzed species (beech and spruce) across the three research networks (AM, FA, MO). Beech recorded lower annual growth values in pure beech stands (FA network), by approximately 15%, compared to those observed in the AM network. This result can be explained by the intensification of intraspecific competition in pure stands compared to mixed stands, where interspecific interactions may lead to more efficient resource utilization. These findings further demonstrate the superiority of mixed stands, predominantly those containing beech, in terms of the growth recorded for this species. For spruce, higher annual growth values (approximately 14%) were recorded in the MO network compared to the AM network; however, the differences observed between the networks were not statistically significant.
  - Regarding the way *competition modifies the relationship between crown parameters and radial growth (TRW),* the results highlighted that the standardized values of the competition index (CIz) were significantly associated with the sociological position of trees, exhibiting a coherent gradient of competition intensity (low, moderate, high). Thus, the relationship between TRW and crown length (CL) revealed an effect dependent on competition intensity, in the sense that its positive influence was more pronounced under conditions of low competition and progressively decreased as

competition intensity increased. In contrast, crown diameter (CD) showed a relatively constant positive effect on radial growth, without significant variation in relation to competition intensity, indicating a stable contribution of CD. At the same time, independently of these relationships, competition intensity exerted a direct and negative effect on radial growth, causing its reduction as competition intensity increased.

*

* *

The research conducted during the preparation of the doctoral thesis and the obtained results highlight that the integrated use of remote sensing data enables not only the accurate estimation of tree dendrometric characteristics, but also the explanation of the mechanisms influencing radial growth in relation to crown dimensions and competition intensity. In this context, the obtained results demonstrate that crown variables have higher explanatory capacity compared to the competition index, with crown length emerging as the main predictor of radial growth, exerting a positive and consistent effect across all analyzed stand types. Crown diameter plays a complementary role, characterized by a more stable influence and lower sensitivity to variations in competition intensity. The analysis of the relationships among crown characteristics indicates that the effect of competition on radial growth is not manifested predominantly through direct mechanisms, but largely through changes occurring at the crown level, particularly through the reduction of crown length. At the same time, the influence of crown length on radial growth progressively decreases under conditions of high competition, whereas the effect of crown diameter remains relatively constant, highlighting differentiated control mechanisms of radial growth. Furthermore, the identified relationships vary according to stand type, being more pronounced in mixed spruce–beech stands compared to pure stands (beech or spruce), indicating a clear dependence on stand structure and composition.

At the same time, the inclusion of tree volume in the analyses represents a logical next step for completing the evaluation of radial growth and productivity, especially through its integration with crown characteristics. Considering tree volume would allow a clearer understanding of tree development processes. In this regard, the inclusion of tree volume in future analyses may contribute to the development of models with broader applicability in forest stand assessment and management.

6. ORIGINAL CONTRIBUTION

During the research conducted for the preparation of the doctoral thesis in forest stands from the western Southern Carpathians, focused on the determination of tree dendrometric characteristics and the analysis of radial growth through the use of integrated data acquired by remote sensing techniques (active and passive sensors). Based on the obtained results and the conclusions drawn, the following original contributions can be formulated:

- ❖ The first development of a unified geospatial database containing common tree-level information specific to forest stands from the western Southern Carpathians, obtained through the integration of remote sensing data acquired by active and passive sensors with field measurements collected through inventories in permanent sample plots.
- ❖ Improvement of the terrestrial laser scanning (TLS) data acquisition process through the implementation of a workflow based on multiple scans (four scan positions) and the uniform distribution of spherical targets, aimed at minimizing occlusion effects at the stem level and within the lower canopy layer, thereby ensuring a more complete stand-level representation.
- ❖ Optimization of the individual tree identification process through the application of a processing workflow based on point cloud segmentation and the integrated use of remote sensing data acquired by active and passive sensors, resulting in precise tree delineation in pure beech stands, pure spruce stands, and mixed beech–spruce stands.
- ❖ The first determination of the contribution of crown variables to explaining radial growth in pure beech stands, pure spruce stands, and mixed beech–spruce stands, highlighting the predominant role of crown length compared to crown diameter within specific models accounting for variation among permanent sample plots.
- ❖ Adoption of a mixed modeling framework integrating both crown length and crown diameter, together with their stand-level interactions, allowing the evaluation of their contribution to radial growth at the individual tree level.
- ❖ The first application of a structural equation model (SEM) in pure beech stands, pure spruce stands, and mixed beech–spruce stands for analyzing the relationships among tree crown characteristics (crown length and crown diameter), the competition index, and radial growth, enabling the evaluation of both direct and indirect effects of competition on radial growth at the individual tree level.
- ❖ Characterization of the way competition among trees modifies the relationship between crown parameters and radial growth by defining and applying three competition intensity levels (low, moderate, high), established according to the percentiles of the competition index (p10, p50, and p90), thereby highlighting variations in radial growth response to changes in crown length and crown diameter.
- ❖ Demonstration that crown length (CL) represents the main indicator through which competition among trees influences radial growth, while crown diameter does not exert a significant direct influence on tree growth and development.
- ❖ The first determination of the direct effect exerted by competition among trees on radial growth through the adoption of two linear mixed models including both tree crown

characteristics and a temporal component (year of observation), and additionally, the competition index and its interaction with the year of observation.

- Identification of the essential role played by crown dimensions in mitigating the effects of competition, demonstrating the capacity of trees with more developed crowns to partially reduce the negative impact of competition on radial growth, particularly under conditions of high stand density.

7. DISSEMINATION OF RESULTS

A. Works related to the doctoral thesis, published in ISI-index journals

1. **CAPALB, F.,** APOSTOL, B., LORENȚ, A., PETRILA, M., MARCU, C., & BADEA, N.O., 2024. Integration of Terrestrial Laser Scanning and field measurements data for tree stem volume estimation: exploring parametric and non-parametric modeling approaches. Annals of Forest Research, Res. 67(1): 77-94. (FI=2,9) (Q1). https://www.afrjournal.org/index.php/afr/article/view/3664/1286

B. Works related to the doctoral thesis, published in BDI-indexed journals

1. **CAPALB, F.,** PETRILA, M., LORENȚ, A., APOSTOL, B., MARCU, C., BADEA, O., 2023. Estimarea volumului la arbori individuali pe baza norilor de puncte obținuți prin scanare cu laser terestru (TLS) – studiu de caz pentru arborete de molid din vestul Carpaților Meridionali (Estimating volume for individual trees based on point clouds obtained through terrestrial laser scanning (TLS) – a case study for spruce stands in the western part of Southern Carpathians). Revista de Silvicultură și Cinegetică Anul XXVIII, nr. 53: 12-18. https://www.revistapadurilor.com/wp-content/uploads/2025/03/53-1.pdf
2. **CAPALB, F.,** APOSTOL, B., CHIVULESCU, S., PETRILA, M, MARCU, C., LORENȚ, A., BADEA, O., 2022. Determinarea înălțimilor arborilor prin intermediul unui model nelinear de predicție, aplicabil arboretelor de molid din vestul Carpaților Meridionali. Revista de Silvicultură și Cinegetică, anul XXVII, nr. 51: 56-61. http://progresulsilvic.ro/numarul-51-al-revistei-de-silvicultura-si-cinegetica

C. Works outside the doctoral thesis domain, published in ISI-indexed journals

1. LORENȚ, A., PETRILA, M., APOSTOL, B., **CAPALB, F.,** CHIVULESCU, Ș., ȘAMȘODAN, C., MARCU, C., BADEA, O., 2025. Assessing and Mapping Forest Fire Vulnerability in Romania Using Maximum Entropy and eXtreme Gradient Boosting. Forests, 16(7), 1156. https://doi.org/10.3390/f16071156
2. CHIVULESCU, S., RADU, R., **CAPALB, F.,** HAPA, I.H., PITAR, D., MARMUREANU, L., LECA, S., PETREA, S., BADEA, N.O., 2023. Cost Valuation and Climate Mitigation Impacts of Forest Management: A Case Study from Piatra Craiului National Park, Romania. Land 13(1):17. https://www.mdpi.com/2073-445X/13/1/17
3. CHIVULESCU, S., CADAR, N., HAPA, I.H., **CAPALB, F.,** RADU, R., BADEA, N.O., 2023. The Necessity of Maintaining the Resilience of Peri-Urban Forests to Secure Environmental and Ecological Balance: A Case Study of Forest Stands Located on the Romanian Sector of the Pannonian Plain. Diversity 15(3):380. https://www.mdpi.com/1424-2818/15/3/380

D. Works outside the doctoral thesis domain, published in BDI-indexed journals

1. PETRILA, M., **CAPALB, F.,** LORENȚ, A., APOSTOL, B., MARCU, C., BADEA, O., 2025. Metodă de evaluare a gradului de vulnerabilitate la doborâturi produse de vânt în ecosisteme forestiere montane. Revista Pădurilor, Volumul 140(4), nr. 3/2025: 3-25.
2. LORENȚ, A., PETRILA, M., APOSTOL, B., **CAPALB, F.,** BIBARȚ, C.,I., BURLUI, I., 2025. Sebastien Lahaye, Domingos Xavier Viegas, Luis Mario Ribeiro, Miguel Almeida, Tiago Rodrigues, Antonio Jorge Ferreira, Ana Isabel Miranda, Diogo Lopes, Tobias Osswald, Johan Sjostrom, Rick McRae, Kiki Yunianti, Fanny Verhilac, 2024. Manual cu instrucțiuni pentru pompieri

pentru a face față incendiilor extreme, incendiilor în zona de interfață natural-construit și incendiilor la latitudini/altitudini mari (Livrabil D2.6, Proiect H2020 FirEUrisk), 93p. Revista Pădurilor, Volumul 140(4), nr. 3/2025: 53-58.

3. **CAPALB, F.,** APOSTOL, B., LORENȚ, A., LECA, Ș., CHIVULESCU, S., PETRILA, M., MARCU, C., BADEA, O., 2025. Posibilități de utilizare a imaginilor hiperspectrale Hyperion pentru identificarea unor specii de arbori. Revista de Silvicultură și Cinegetică Anul XXIX, nr. 56: 12-20. https://www.progresulsilvic.ro/wp-content/uploads/2025/09/2025.56.pdf
4. LORENȚ, A., PETRILA, M., **CAPALB, F.,** APOSTOL, B., MARCU, C., BADEA, O., 2024. Overview of the Forest Fires Defense System in Romania. In: Dobrinkova, N., Fidanova, S. (eds) Environmental Protection and Disaster Risks (EnviroRisks 2024). EnviroRISKs 2024. Lecture Notes in Networks and Systems, vol 883. Springer, Cham. https://doi.org/10.1007/978-3-031-74707-6_29
5. LORENȚ, A., GANCZ, V., PETRILA, M., APOSTOL, B., **CAPALB, F.,** MARCU, C., BADEA, O., 2023. Detection and localization of forest fires and tracking their evolution based on high temporal resolution satellite images (Detectarea și localizarea incendiilor de pădure și urmărirea evoluției acestora pe baza imaginilor satelitare de înaltă rezoluție temporală). Revista de Silvicultură și Cinegetică Anul XXVIII, nr. 52: 63-69. http://progresulsilvic.ro/a-aparut-numarul-52-al-revistei-de-silvicultura-si-cinegetica-il-puteti-descarca-in-format-pdf

E. Participation in International Conferences

1. **CAPALB, F.,** PETRILA, M., APOSTOL, B., LORENȚ, A., MARCU, C., BADEA, O., 2025. A Comparative Analysis of TLS and MLS Technologies for Estimation of Dendrometric Tree Characteristics in Mixed Temperate Forests. Silvilaser 2025, Quebec, Canada, 29 September – 3 October 2025. *(prezentare)*
2. **CAPALB, F.,** APOSTOL, B., LORENȚ, A., PETRILA, M., MARCU, C., BADEA, O., 2025. Combining Terrestrial Laser Scanning and Field Measurements for Estimating Tree Stem Volume. COST Action CA20118 - 3DForEcoTech Final conference.Three-dimensional forest ecosystem monitoring and better understanding by terrestrial-based technologies. Forest Research Institute, Sękocin Stary, Poland, 2-4 July 2025. *(poster)*
3. LORENȚ, A., PETRILA, M., **CAPALB, F.,** APOSTOL, B., MARCU, C., BADEA, O., 2024. Overview of the Forest Fires Defense System in Romania. EnviroRISKs 2024 – 12th CMDR-COE Annual Conference on Crisis Management and Disaster Response and 3rd International Conference on ENVIROnmental Protection and Disaster Risks, 4 – 6 iunie 2024, Sofia, Bulgaria. *(prezentare)*
4. PETRILA, M., **CAPALB, F.,** LORENȚ, A., APOSTOL, B., MARCU, C., BADEA, O., 2024. A Comparative Analysis of TLS and GeoSLAM Technologies for Forest Monitoring. Integrating biodiversity conservation in forest management - Final Conference COST Action CA18207-Biodiversity Of Temperate forest Taxa Orienting Management Sustainability by Unifying Perspectives (BOTTOMS-UP) 19-21 March 2024, Botanical Garden, Rome, Italy. *(poster)*
5. COULIBALY, F., APOSTOL, B., PASCU, I.S., **CAPALB, F.,** SICARD, P., BADEA O., 2023. Urban Trees Detection Using Very High-Resolution Satellite Imagery – Smart Solution for

Municipal Green Cadaster. Forest science for people and societal challenges - The 90th "Marin Drăcea" INCDS Anniversary, 2-5 octombrie 2023, București, România. *(prezentare)*

6. **CAPALB, F.,** PETRILA, M., LORENȚ, A., APOSTOL, B., MARCU, C., BADEA, O., 2023. Predicting Tree Crown Width of Individual Trees In The Western Southern Carpathians Using Terrestrial Laser Scanning And Random Forest Algorithm. Forest science for people and societal challenges - The 90th "Marin Drăcea" INCDS Anniversary, 2-5 octombrie 2023, București, România. *(prezentare)*
7. **CAPALB, F.,** PETRILA, M., LORENȚ, A., APOSTOL, B., MARCU, C., BADEA, O., 2023. Experimenting an improved tree point cloud segmentation method of TLS data in a spruce forest inventory network. SilviLaser 2023, Londra, UK, 6-8 septembrie 2023. *(poster)*
8. LORENT A., PETRILA M., APOSTOL B., **CAPALB F.,** MARCU C., BADEA O., 2023. Identification Of The Driving Factors For The Occurrence Of Forest Fires And The Zoning Of Forest Fire Hazard Through Logistic Regression And Random Forest In Romania Fire Hazard Through Logistic Regression and Random Forest in Romania, al 42-lea simpozion EARSeL, Bucuresti, Romania, 3-6 iulie 2023. *(prezentare)*
9. APOSTOL B., LORENȚ A., CHIVULESCU Ș., CICEU A., PETRILA M., **CAPALB F.,** MARCU C., BADEA O., 2022. Integration of Terrestrial Laser Scanning (TLS) and Airborne Laser Scanning (ALS) Processed Data for the Assessment of Norway Spruce Dendrometric Characteristics – a Case Study, al 41-lea simpozion EARSeL, Paphos, Cipru, 13-16 septembrie 2022. *(poster)*
10. APOSTOL B., PETRILA M., DURO J.G., LORENȚ A., **CAPALB F.,** MARCU C., FARCAȘ S., 2022. Integration of Canopy Height Models Derived from Airborne LiDAR Data and UAV Aerial Imagery by DTM-DSM Matching in the Forest Free Areas, al 41-lea simpozion EARSeL, Paphos, Cipru, 13-16 septembrie 2022. *(poster)*
11. LORENȚ A., GANCZ V., PETRILA M., **CAPALB F.,** APOSTOL B., SOARE I., 2022. A web GIS mapping service for a better exploitation of the forest melliferous resources in South East Romania, al 41-lea simpozion EARSeL, Paphos, Cipru, 13-16 septembrie 2022. *(poster)*

LIST OF TABLES

LIST OF FIGURES

BIBLIOGRAPHY

Abegg M., Bösch R., Kükenbrink D., Morsdorf F., 2023. Tree volume estimation with terrestrial laser scanning — Testing for bias in a 3D virtual environment. Agricultural and Forest Meteorology 331: . https://doi.org/10.1016/j.agrformet.2023.109348

Agisoft LLC, 2021. Agisoft Metashape User Manual Professional Edition, Version 1.7. Agisoft Metashape (September): .

Ahmed S., Hilmers T., Uhl E., Tupinambá-Simões F., Bravo F., del Río M., Pretzsch H., 2025. Crown structure indicates tree secondary growth, competition legacy, and growth potential of dominant species in Europe. Ecological Indicators 170(December 2024): . https://doi.org/10.1016/j.ecolind.2025.113074

Ahmed S., Pretzsch H., 2023. TLidar-based crown shape indicates tree ring pattern in Norway spruce (Picea abies (L.) H. Karst) trees across competition gradients. A modeling and methodological approach. Ecological Indicators 148: . https://doi.org/10.1016/j.ecolind.2023.110116

Apostol B., Chivulescu S., Ciceu A., Petrila M., Pascu I.S., Apostol E.N., Leca Ș., Lorenț A., Tănase M., Badea O., 2018. Data collection methods for forest inventory: A comparison between an integrated conventional equipament and terrestrial laser scanning. Annals of Forest Research 61(2): . https://doi.org/10.15287/afr.2018.1189

Arrizza S., Marras S., Ferrara R., Pellizzaro G., 2024. Terrestrial Laser Scanning (TLS) for tree structure studies: a review of methods for wood-leaf classifications from 3D point clouds. Remote Sensing Applications: Society and Environment 36(September): 101364. https://doi.org/10.1016/j.rsase.2024.101364

Badea O., 2008. *Manual privind metodologia de supraveghere pe termen lung a stării ecosistemelor forestiere aflate sub acțiunea poluării atmosferice și modificărilor climatice*. Bucharest: Editura Silvică.

Badea O., 2013. *Cercetări ecologice pe termen scurt în ecosisteme forestiere reprezentative din Parcul Natural Bucegi*. i. Badea, O. (ed.). Editura Silvică.

Ball J.G.C., Hickman S.H.M., Jackson T.D., Koay X.J., Hirst J., Jay W., Archer M., Aubry-Kientz M., Vincent G., Coomes D.A., 2023. Accurate delineation of individual tree crowns in tropical forests from aerial RGB imagery using Mask R-CNN. Remote Sensing in Ecology and Conservation 9(5): . https://doi.org/10.1002/rse2.332

Bates D., Mächler M., Bolker B., Walker S., 2015. Fitting Linear Mixed-Effects Models Using lme4. Journal of Statistical Software 67(1 SE-Articles): 1–48. https://doi.org/10.18637/jss.v067.i01

Bayer D., Seifert S., Pretzsch H., 2013. Structural crown properties of Norway spruce (Picea abies [L.] Karst.) and European beech (Fagus sylvatica [L.]) in mixed versus pure stands revealed by terrestrial laser scanning. Trees - Structure and Function 27(4): . https://doi.org/10.1007/s00468-013-0854-4

Bazezew M.N., Hussin Y.A., Kloosterman E.H., 2018. Integrating Airborne LiDAR and Terrestrial Laser Scanner forest parameters for accurate above-ground biomass/carbon estimation in Ayer Hitam tropical forest, Malaysia. International Journal of Applied Earth Observation and Geoinformation 73: . https://doi.org/10.1016/j.jag.2018.07.026

Beloiu M., Heinzmann L., Rehush N., Gessler A., Griess V.C., 2023. Individual Tree-Crown Detection and Species Identification in Heterogeneous Forests Using Aerial RGB Imagery and Deep Learning. Remote Sensing 15(5): . https://doi.org/10.3390/rs15051463

Bienert A., Georgi L., Kunz M., Maas H.G., von Oheimb G., 2018. Comparison and combination of mobile and terrestrial laser scanning for natural forest inventories. Forests 8(2): . https://doi.org/10.3390/f9070395

Bogdanovich E., Perez-Priego O., El-Madany T.S., Guderle M., Pacheco-Labrador J., Levick S.R., Moreno G., Carrara A., Pilar Martín M., Migliavacca M., 2021. Using terrestrial laser scanning for characterizing tree structural parameters and their changes under different management in a Mediterranean open woodland. Forest Ecology and Management 486: . https://doi.org/10.1016/j.foreco.2021.118945

Bornand A., Rehush N., Morsdorf F., Thürig E., Abegg M., 2023. Individual tree volume estimation with terrestrial laser scanning: Evaluating reconstructive and allometric approaches. Agricultural and Forest Meteorology 341: . https://doi.org/10.1016/j.agrformet.2023.109654

Bunn A.G., 2008. A dendrochronology program library in R (dplR). Dendrochronologia 26(2): . https://doi.org/10.1016/j.dendro.2008.01.002

Calders K., Adams J., Armston J., Bartholomeus H., Bauwens S., Bentley L.P., Chave J., Danson F.M., Demol M., Disney M., Gaulton R., Krishna Moorthy S.M., Levick S.R., Saarinen N., Schaaf C., Stovall A., Terryn L., Wilkes P., Verbeeck H., 2020. Terrestrial laser scanning in forest ecology: Expanding the horizon. *Remote Sensing of Environment*. 251. https://doi.org/10.1016/j.rse.2020.112102

Campelo F., García-González I., Nabais C., 2012. DetrendeR - A Graphical User Interface to process and visualize tree-ring data using R. Dendrochronologia 30(1): . https://doi.org/10.1016/j.dendro.2011.01.010

Chen J., Zhao D., Zheng Z., Xu C., Pang Y., Zeng Y., 2024. A clustering-based automatic registration of UAV and terrestrial LiDAR forest point clouds. Computers and Electronics in Agriculture 217: . https://doi.org/10.1016/j.compag.2024.108648

Chifunda E.F., Kirigiti P.J., Balan R.T., 2025. Modelling tree-level aboveground biomass and carbon stock in Tanzania's Miombo Woodlands incorporating spectral indices using machine learning algorithms. Environmental Research Communications 7(10): . https://doi.org/10.1088/2515-7620/ae0ac9

Chivulescu S., Ciceu A., Leca S., Apostol B., Popescu O., Badea O., 2020. Development phases and structural characteristics of the Penteleu-Viforta virgin forest in the Curvature Carpathians. iForest - Biogeosciences and Forestry (5): 389–395. https://doi.org/10.3832/ifor3094-013

Collazos Fernández E., Rubiales J.M., 2025. Reconstruction of Torrential Activity in Cerradillas Valley (Sierra de Guadarrama National Park, Spain) Using Dendrogeomorphic Techniques. Geosciences (Switzerland) 15(10): . https://doi.org/10.3390/geosciences15100402

Compeán-Aguirre J.L., López-Serrano P.M., Silván-Cárdenas J.L., Martínez-García-Moreno C.A., Vega-Nieva D.J., Corral-Rivas J.J., Pompa-García M., 2024. Evaluation of Two-Dimensional DBH Estimation Algorithms Using TLS. Forests 15(11): . https://doi.org/10.3390/f15111964

Corte A.P.D., Souza D.V., Rex F.E., Sanquetta C.R., Mohan M., Silva C.A., Zambrano A.M.A., Prata G., Alves de Almeida D.R., Trautenmüller J.W., Klauberg C., de Moraes A., Sanquetta M.N., Wilkinson B., Broadbent E.N., 2020. Forest inventory with high-density UAV-Lidar: Machine learning approaches for predicting individual tree attributes. Computers and Electronics in Agriculture 179: . https://doi.org/10.1016/j.compag.2020.105815

Demol M., Verbeeck H., Gielen B., Armston J., Burt A., Disney M., Duncanson L., Hackenberg J., Kükenbrink D., Lau A., Ploton P., Sewdien A., Stovall A., Takoudjou S.M., Volkova L., Weston C., Wortel V., Calders K., 2022. Estimating forest above-ground biomass with terrestrial laser scanning: Current status and future directions. *Methods in Ecology and Evolution*. 13 (8).

https://doi.org/10.1111/2041-210X.13906
Dinca L., Nita M.D., Hofgaard A., Alados C.L., Broll G., Borz S.A., Wertz B., Monteiro A.T., 2017. Forests dynamics in the montane-alpine boundary: A comparative study using satellite imagery and climate data. Climate Research 73(1–2): . https://doi.org/10.3354/cr01452
Dobre A.C., Pascu I.S., Leca Ștefan, Garcia-Duro J., Dobrota C.E., Tudoran G.M., Badea O., 2021. Applications of tls and als in evaluating forest ecosystem services: A southern carpathians case study. Forests 12(9): . https://doi.org/10.3390/f12091269
Dubayah R., Blair J.B., Goetz S., Fatoyinbo L., Hansen M., Healey S., Hofton M., Hurtt G., Kellner J., Luthcke S., Armston J., Tang H., Duncanson L., Hancock S., Jantz P., Marselis S., Patterson P.L., Qi W., Silva C., 2020. The Global Ecosystem Dynamics Investigation: High-resolution laser ranging of the Earth's forests and topography. Science of Remote Sensing 1: . https://doi.org/10.1016/j.srs.2020.100002
European Environmnet Agency (EEA), 2020. Copernicus Land Monitoring Service 2020. European Environment Agency (EEA)
Fan G., Nan L., Dong Y., Su X., Chen F., 2020. AdQSM: A new method for estimating above-ground biomass from TLS point clouds. Remote Sensing 12(18): . https://doi.org/10.3390/RS12183089
FARO Technologies Inc, 2019.
Fox J., Weisberg S., Price B., Adler D., Bates D., Baud-bovy G., Bolker B., Ellison S., Firth D., Friendly M., Gorjanc G., Graves S., Heiberger R., Laboissiere R., Maechler M., Monette G., Murdoch D., Nilsson H., Ogle D., Ripley B., Venables W., Walker S., Winsemius D., Zeileis A., R-Core, 2021. Package 'car': Companion to Applied Regression. CRAN Repository
García M., Danson F.M., Riaño D., Chuvieco E., Ramirez F.A., Bandugula V., 2011. Terrestrial laser scanning to estimate plot-level forest canopy fuel properties. International Journal of Applied Earth Observation and Geoinformation 13(4): . https://doi.org/10.1016/j.jag.2011.03.006
Giannetti F., Puletti N., Quatrini V., Travaglini D., Bottalico F., Corona P., Chirici G., 2018. Integrating terrestrial and airborne laser scanning for the assessment of single-tree attributes in Mediterranean forest stands. European Journal of Remote Sensing 51(1): . https://doi.org/10.1080/22797254.2018.1482733
Giurgiu V., 1979. *Dendrometrie și auxologie forestieră*. Ceres.
Giurgiu V., Decei I., Draghiciu D., 2004. *Metode și tabele dendrometrice*. București: Editura Ceres.
Griese N., Ritzert M., Nölke N., 2025. A large dataset of labelled single tree point clouds, QSMs and tree graphs. Scientific Data 12(1): . https://doi.org/10.1038/s41597-025-06421-7
Han T., Sánchez-Azofeifa G.A., 2022. Extraction of Liana Stems Using Geometric Features from Terrestrial Laser Scanning Point Clouds. Remote Sensing 14(16): . https://doi.org/10.3390/rs14164039
He M., Hu Y., Zhao J., Li Y., Wang B., Zhang J., Noguchi H., 2025. Exploring Stand Parameters Using Terrestrial Laser Scanning in Pinus tabuliformis Plantation Forests. Remote Sensing 17(7): . https://doi.org/10.3390/rs17071228
Henrich J., van Delden J., Seidel D., Kneib T., Ecker A.S., 2024. TreeLearn: A deep learning method for segmenting individual trees from ground-based LiDAR forest point clouds. Ecological Informatics 84: . https://doi.org/10.1016/j.ecoinf.2024.102888
Holvoet J., Eichhorn M.P., Giannetti F., Kükenbrink D., Liang X., Mokroš M., Novotný J., Pitkänen T.P., Puliti S., Skudnik M., Stereńczak K., Terryn L., Vega C., Torresan C., 2025. Terrestrial and mobile laser scanning for national forest inventories: From theory to implementation. Remote Sensing

of Environment 329(August 2024): . https://doi.org/10.1016/j.rse.2025.114947

Iglhaut J., Cabo C., Puliti S., Piermattei L., O'Connor J., Rosette J., 2019. Structure from Motion Photogrammetry in Forestry: a Review. *Current Forestry Reports*. 5 (3). https://doi.org/10.1007/s40725-019-00094-3

Jacob J., Varadharajan R., 2024. Robust Variance Inflation Factor: A Promising Approach for Collinearity Diagnostics in the Presence of Outliers. Sankhya B 86(2): . https://doi.org/10.1007/s13571-024-00342-y

Jiang H., Hu R., Yan G., Cheng S., Li F., Qi J., Li L., Xie D., Mu X., 2021. Influencing factors in estimation of leaf angle distribution of an individual tree from terrestrial laser scanning data. Remote Sensing 13(6): . https://doi.org/10.3390/rs13061159

Jucker T., Fischer F.J., Chave J., Coomes D.A., Caspersen J., Ali A., Loubota Panzou G.J., Feldpausch T.R., Falster D., Usoltsev V.A., Jackson T.D., Adu-Bredu S., Alves L.F., Aminpour M., Angoboy Ilondea B., Anten N.P.R., Antin C., Askari Y., Ayyappan N., Banin L.F., Barbier N., Battles J.J., Beeckman H., Bocko Y.E., Bond-Lamberty B., Bongers F., Bowers S., van Breugel M., Chantrain A., Chaudhary R., Dai J., Dalponte M., Dimobe K., Domec J.C., Doucet J.L., Dupuy Rada J.M., Duursma R.A., Enríquez M., van Ewijk K.Y., Farfán-Rios W., Fayolle A., Ferretti M., Forni E., Forrester D.I., Gilani H., Godlee J.L., Haeni M., Hall J.S., He J.K., Hemp A., Hernández-Stefanoni J.L., Higgins S.I., Holdaway R.J., Hussain K., Hutley L.B., Ichie T., Iida Y., Jiang H.S., Joshi P.R., Kaboli H., Kazempour Larsary M., Kenzo T., Kloeppel B.D., Kohyama T.S., Kunwar S., Kuyah S., Kvasnica J., Lin S., Lines E.R., Liu H., Lorimer C., Loumeto J.J., Malhi Y., Marshall P.L., Mattsson E., Matula R., Meave J.A., Mensah S., Mi X., Momo S.T., Moncrieff G.R., Mora F., Muñoz R., Nissanka S.P., Nur Hajar Z.S., O'Hara K.L., Pearce S., Pelissier R., Peri P.L., Ploton P., Poorter L., Pour M.J., Pourbabaei H., Ribeiro S.C., Ryan C., Sanaei A., Sanger J., Schlund M., Sellan G., Shenkin A., Sonké B., Sterck F.J., Svátek M., Takagi K., Trugman A.T., Vadeboncoeur M.A., Valipour A., Vanderwel M.C., Vovides A.G., Waldner P., Wang W., Wang L.Q., Wirth C., Woods M., Xiang W., de Aquino Ximenes F., Xu Y., Yamada T., Zavala M.A., Zimmermann N.E., 2025. The global spectrum of tree crown architecture. Nature Communications 16(1): 45–50. https://doi.org/10.1038/s41467-025-60262-x

Keskes M.I., Mohamed A.H., Borz S.A., Niță M.D., 2025. Improving National Forest Mapping in Romania Using Machine Learning and Sentinel-2 Multispectral Imagery. Remote Sensing 17(4): . https://doi.org/10.3390/rs17040715

Kröner K., Larysch E., Schindler Z., Obladen N., Frey J., Stangler D.F., Seifert T., 2024. Influence of crown morphology and branch architecture on tree radial growth of drought-affected Fagus sylvatica L. Forest Ecosystems 11(August): . https://doi.org/10.1016/j.fecs.2024.100237

Kuznetsova A., Brockhoff P.B., Christensen R.H.B., 2017. lmerTest Package: Tests in Linear Mixed Effects Models. Journal of Statistical Software 82(13): . https://doi.org/10.18637/JSS.V082.I13

Labrecque-Foy J.P., Angers-Blondin S., Ropars P., Simard M., Boudreau S., 2023. The Use of Basal Area Increment to Preserve the Multi-Decadal Climatic Signal in Shrub Growth Ring Chronologies: A Case Study of Betula glandulosa in a Rapidly Warming Environment. Atmosphere 14(2): . https://doi.org/10.3390/atmos14020319

Liang X., Kankare V., Hyyppä J., Wang Y., Kukko A., Haggrén H., Yu X., Kaartinen H., Jaakkola A., Guan F., Holopainen M., Vastaranta M., 2016. Terrestrial laser scanning in forest inventories. ISPRS Journal of Photogrammetry and Remote Sensing 115: . https://doi.org/10.1016/j.isprsjprs.2016.01.006

Maas H.G., Bienert A., Scheller S., Keane E., 2008. Automatic forest inventory parameter determination from terrestrial laser scanner data. In: *International Journal of Remote Sensing*. 2008 p.

https://doi.org/10.1080/01431160701736406
Mîzgaciu L., Tudoran G.M., Ciocan A.E., Stăncioiu P.T., Niță M.D., 2025. A Comparative Analysis of UAV LiDAR and Mobile Laser Scanning for Tree Height and DBH Estimation in a Structurally Complex, Mixed-Species Natural Forest. Forests 16(9): 1–21. https://doi.org/10.3390/f16091481
Mohan M., Silva C.A., Klauberg C., Jat P., Catts G., Cardil A., Hudak A.T., Dia M., 2017. Individual tree detection from unmanned aerial vehicle (UAV) derived canopy height model in an open canopy mixed conifer forest. Forests 8(9): . https://doi.org/10.3390/f8090340
Nasiri V., Darvishsefat A.A., Arefi H., Pierrot-Deseilligny M., Namiranian M., Le Bris A., 2021. Unmanned aerial vehicles (Uav)-based canopy height modeling under leaf-on and leaf-off conditions for determining tree height and crown diameter (case study: Hyrcanian mixed forest). *Canadian Journal of Forest Research*. 51 (7). https://doi.org/10.1139/cjfr-2020-0125
Niță M.D., 2021. Testing forestry digital twinning workflow based on mobile lidar scanner and ai platform. Forests 12(11): . https://doi.org/10.3390/f12111576
Olivier M.D., Robert S., Fournier R.A., 2016. Response of sugar maple (Acer saccharum, Marsh.) tree crown structure to competition in pure versus mixed stands. Forest Ecology and Management 374: . https://doi.org/10.1016/j.foreco.2016.04.047
Olofsson K., Holmgren J., Olsson H., 2014. Tree stem and height measurements using terrestrial laser scanning and the RANSAC algorithm. Remote Sensing 6(5): . https://doi.org/10.3390/rs6054323
Onishi M., Ise T., 2021. Explainable identification and mapping of trees using UAV RGB image and deep learning. Scientific Reports 11(1): . https://doi.org/10.1038/s41598-020-79653-9
Pascu I.S., Dobre A.C., Badea O., Tanase M.A., 2020. Retrieval of forest structural parameters from terrestrial laser scanning: A Romanian case study. Forests 11(4): . https://doi.org/10.3390/F11040392
Pascu I.S., Dobre A.C., Badea O., Tănase M.A., 2019. Estimating forest stand structure attributes from terrestrial laser scans. Science of the Total Environment 691: . https://doi.org/10.1016/j.scitotenv.2019.06.536
Penanhoat A., Guerrero Ramirez N., Aubry-Kientz M., Diekmann L., Paligi S., Audisio M., Mrak K., Seidel D., 2024. Effect of competition intensity and neighbor identity on architectural traits of Fagus sylvatica. Trees - Structure and Function 38(5): 1177–1187. https://doi.org/10.1007/s00468-024-02544-3
Perles-Garcia M.D., Kunz M., Fichtner A., Meyer N., Härdtle W., von Oheimb G., 2022. Neighbourhood Species Richness Reduces Crown Asymmetry of Subtropical Trees in Sloping Terrain. Remote Sensing 14(6): . https://doi.org/10.3390/rs14061441
Petrila M., Apostol B., Lorenț A., Gancz V., Silaghi D., 2012. Forest biomass estimation by the use of airborne laser scanning data and in situ FieldMap measurements in a spruce forest stand. Folia Forestalia Polonica, Series A 54(2): .
Picos J., Bastos G., Míguez D., Alonso L., Armesto J., 2020. Individual tree detection in a eucalyptus plantation using unmanned aerial vehicle (UAV)-LiDAR. Remote Sensing 12(5): . https://doi.org/10.3390/rs12050885
Pikiński P., Szaban J., Šilingienė G., Korzeniewicz R., Pazdrowski W., 2021. Selected physical and mechanical properties of scots pine (Pinus sylvestris l.) wood from stands of younger age classes as criteria for rational utilization of timber. Baltic Forestry 27(1): . https://doi.org/10.46490/BF363
Pitkänen T.P., Raumonen P., Liang X., Lehtomäki M., Kangas A., 2021. Improving TLS-based stem

volume estimates by field measurements. Computers and Electronics in Agriculture 180: . https://doi.org/10.1016/j.compag.2020.105882

Posit team, 2025.

Pretzsch H., 2021. Tree growth as affected by stem and crown structure. Trees - Structure and Function 35(3): . https://doi.org/10.1007/s00468-021-02092-0

Purves D.W., Lichstein J.W., Pacala S.W., 2007. Crown plasticity and competition for canopy space: A new spatially implicit model parameterized for 250 North American tree species. PLoS ONE 2(9): . https://doi.org/10.1371/journal.pone.0000870

R Core Team, 2025.

Rieder J.S., Link R.M., Köthe K., Seidel D., Ullmann T., Žmegač A., Zang C., Schuldt B., 2024. TreeCompR: Tree competition indices for inventory data and 3D point clouds. Methods in Ecology and Evolution 15(12): . https://doi.org/10.1111/2041-210X.14414

Roussel J.-R., 2025.

Salmerón-Gómez R., García-García C.B., García-Pérez J., 2025. A Redefined Variance Inflation Factor: Overcoming the Limitations of the Variance Inflation Factor. Computational Economics 65(1): . https://doi.org/10.1007/s10614-024-10575-8

Schneider F.D., Kükenbrink D., Schaepman M.E., Schimel D.S., Morsdorf F., 2019. Quantifying 3D structure and occlusion in dense tropical and temperate forests using close-range LiDAR. Agricultural and Forest Meteorology 268: . https://doi.org/10.1016/j.agrformet.2019.01.033

Shang C., Treitz P., Caspersen J., Jones T., 2019. Estimation of forest structural and compositional variables using ALS data and multi-seasonal satellite imagery. International Journal of Applied Earth Observation and Geoinformation 78: . https://doi.org/10.1016/j.jag.2018.10.002

Shrestha N., 2020. Detecting Multicollinearity in Regression Analysis. American Journal of Applied Mathematics and Statistics 8(2): . https://doi.org/10.12691/ajams-8-2-1

Signorell A, Aho K, Alfons A, Anderegg N, Aragon T, Arachchige C, ve ark, 2024. R Package 'DescTools'. Tools for Descriptive Statistics. https://cran.r-project.org/ 0.99.54: .

So K., Chau J., Rudd S., Robinson D.T., Chen J., Cyr D., Gonsamo A., 2025. Direct Estimation of Forest Aboveground Biomass from UAV LiDAR and RGB Observations in Forest Stands with Various Tree Densities. Remote Sensing 17(12): 1–17. https://doi.org/10.3390/rs17122091

Solano F., Modica G., Praticò S., Box O.F., Piovesan G., 2022. Unveiling the complex canopy spatial structure of a Mediterranean old-growth beech (Fagus sylvatica L.) forest from UAV observations. Ecological Indicators 138: . https://doi.org/10.1016/j.ecolind.2022.108807

Srinivasan S., Popescu S.C., Eriksson M., Sheridan R.D., Ku N.W., 2015. Terrestrial laser scanning as an effective tool to retrieve tree level height, crown width, and stem diameter. Remote Sensing 7(2): . https://doi.org/10.3390/rs70201877

Terryn L., Calders K., Åkerblom M., Bartholomeus H., Disney M., Levick S., Origo N., Raumonen P., Verbeeck H., 2023. Analysing individual 3D tree structure using the R package ITSMe. Methods in Ecology and Evolution 14(1): . https://doi.org/10.1111/2041-210X.14026

Terryn L., Calders K., Bartholomeus H., Bartolo R.E., Brede B., D'hont B., Disney M., Herold M., Lau A., Shenkin A., Whiteside T.G., Wilkes P., Verbeeck H., 2022. Quantifying tropical forest structure through terrestrial and UAV laser scanning fusion in Australian rainforests. Remote Sensing of Environment 271: . https://doi.org/10.1016/j.rse.2022.112912

Tudoran G.-M., 2022. Using Mathematical Models Based On Unmanned Aerial Vehicle Optical Imagery to Estimate Tree and Stand Characteristics. Bulletin of the Transilvania University of Brasov.

Series I - Engineering Sciences https://doi.org/10.31926/but.ens.2022.15.64.1.5
Vorovencii I., 2024. Assessing Various Scenarios of Multitemporal Sentinel-2 Imagery, Topographic Data, Texture Features, and Machine Learning Algorithms for Tree Species Identification. IEEE Journal of Selected Topics in Applied Earth Observations and Remote Sensing 17: 15373–15392. https://doi.org/10.1109/JSTARS.2024.3436624
Wallace L., Lucieer A., Malenovskỳ Z., Turner D., Vopěnka P., 2016. Assessment of forest structure using two UAV techniques: A comparison of airborne laser scanning and structure from motion (SfM) point clouds. Forests 7(3): . https://doi.org/10.3390/f7030062
Wang D., Liang X., Mofack G.I., Martin-Ducup O., 2021. Individual tree extraction from terrestrial laser scanning data via graph pathing. Forest Ecosystems 8(1): . https://doi.org/10.1186/s40663-021-00340-w
Weiser H., Schäfer J., Winiwarter L., Krašovec N., Fassnacht F.E., Höfle B., 2022. Individual tree point clouds and tree measurements from multi-platform laser scanning in German forests. Earth System Science Data 14(7): . https://doi.org/10.5194/essd-14-2989-2022
Wezyk P., Koziol K., Glista M., Pierzchalski M., 2007. Terrestrial laser scanning versus traditional forest inventory first results from the polish forests. In: *ISPRS Workshop on Laser Scanning 2007 and SilviLaser 2007, Finland*. 2007 p.
White J.C., Coops N.C., Wulder M.A., Vastaranta M., Hilker T., Tompalski P., 2016. Remote Sensing Technologies for Enhancing Forest Inventories: A Review. *Canadian Journal of Remote Sensing*. 42 (5). https://doi.org/10.1080/07038992.2016.1207484
Wielgosz M., Puliti S., Xiang B., Schindler K., Astrup R., 2024. SegmentAnyTree: A sensor and platform agnostic deep learning model for tree segmentation using laser scanning data. Remote Sensing of Environment 313: . https://doi.org/10.1016/j.rse.2024.114367
Xiang B., Wielgosz M., Kontogianni T., Peters T., Puliti S., Astrup R., Schindler K., 2024. Automated forest inventory: Analysis of high-density airborne LiDAR point clouds with 3D deep learning. Remote Sensing of Environment 305: . https://doi.org/10.1016/j.rse.2024.114078
Zeferino S.L., Gama N.C., Souza D.V., de Souza A.S., Ruz E.J.H., da Silva S.D.B., 2023. Generalized Linear Models for Describing Tree Gaps in Forest Management Areas in the Brazilian Amazon. Forests 14(4): . https://doi.org/10.3390/f14040841
Zhang Y., Liao J., Xu C., Du M., Zhang X., 2024. Optimizing variables selection of random forest to predict radial growth of Larix gmelinii var. principis-rupprechtii in temperate regions. Forest Ecology and Management 569: . https://doi.org/10.1016/j.foreco.2024.122159
Zhou R., Sun H., Ma K., Tang J., Chen S., Fu L., Liu Q., 2023. Improving Estimation of Tree Parameters by Fusing ALS and TLS Point Cloud Data Based on Canopy Gap Shape Feature Points. Drones 7(8): . https://doi.org/10.3390/drones7080524
Zhu Z., Kleinn C., Nölke N., 2020. Towards tree green crown volume: A methodological approach using terrestrial laser scanning. *Remote Sensing*. 12 (11). https://doi.org/10.3390/rs12111841

SHORT ABSTRACT RO

Cercetările efectuate cu ocazia elaborării prezentei teze de doctorat au avut drept scop fundamentarea științifică și aplicarea tehnicilor de teledetecție privind utilizarea integrată a datelor achiziționate de senzori activi și pasivi cu măsurătorile din teren efectuate prin inventarieri în suprafețe de probă permanente, pentru determinarea caracteristicilor dendrometrice ale arborilor și ale coroanelor acestora și analiza creșterii radiale, în arborete din vestul Carpaților Meridionali. În acest sens, au fost analizate un număr de 96 sondaje permanente aparținând unor tipuri diferite de arborete (amestecate și pure), utilizând date obținute prin scanarea cu laser terestru (TLS) și platforme UAV, în vederea estimării parametrilor dimensionali ai arborilor și a caracteristicilor coroanei, precum și pentru evaluarea relațiilor dintre creșterea radială și intensitatea competiției. Rezultatele obținute au evidențiat faptul că procesul de coregistrare a norilor de puncte se realizează, în majoritatea cazurilor, în limite reduse ale erorilor de coregistrare, fiind influențat în principal de gradul de suprapunere între scanări și de complexitatea structurală a arboretelor. De asemenea, s-a constatat faptul că acuratețea detecției arborilor scade odată cu creșterea desimii arboretului, pe fondul suprapunerii coroanelor arborilor și al creșterii frecvenței omisiunilor. Estimarea diametrului de bază a indicat o concordanță ridicată cu valorile de referință, măsurate în teren, confirmând stabilitatea metodei în condiții variate, în timp ce estimarea înălțimii arborilor a fost afectată de limitări specifice scanării cu laser terestru, în special de efectele de ocluzie, limitări care au fost diminuate prin integrarea datelor UAV. Analiza relațiilor dintre creșterea radială, caracteristicile coroanei arborilor și competiție a evidențiat faptul că dimensiunile coroanei au un rol determinant în explicarea variației creșterii radiale, lungimea coroanei evidențiindu-se ca principal predictor, în timp ce diametrul coroanei are un rol complementar, iar indicele de competiție o contribuție mai redusă. În același timp, s-a pus în evidență faptul că efectul competiției asupra creșterii radiale nu este exclusiv direct, ci se manifestă în mare parte prin modificarea dimensiunilor coroanei, în special prin reducerea lungimii acesteia. Totodată, relațiile identificate variază în raport cu tipul de arboret, fiind mai pronunțate în arboretele de amestec (molid cu fag) comparativ cu cele pure (fag, molid). Modelele utilizate au confirmat capacitatea caracteristicilor coroanei de a explica dinamica creșterii radiale. Rezultatele obținute evidențiază potențialul utilizării integrate a datelor de teledetecție achiziționate de senzori activi și pasivi în determinarea caracteristicilor dendrometrice ale arborilor și analiza creșterii radiale a acestora.

SHORT ABSTRACT EN

The research conducted within the framework of this doctoral thesis aimed at the scientific substantiation and application of remote sensing techniques, focusing on the integrated use of data acquired by active and passive sensors together with field measurements obtained through forest inventories in permanent sample plots, for the determination of tree dendrometric characteristics and crown attributes, as well as for the analysis of radial growth in forest stands located in the part of the Southern Carpathians. In this context, a total of 96 permanent sample plots across to different types of stands (mixed and pure) were analyzed, using data obtained from terrestrial laser scanning (TLS) and UAV platforms, with the aim of estimating tree dimensional parameters and crown characteristics, as well as assessing the relationships between radial growth and competition intensity. The results showed that the co-registration process of point clouds is generally achieved within low error limits, being mainly influenced by the degree of overlap between scans and structural complexity of the stands. It was also found that tree detection accuracy decreases with increasing stand density, due to crown overlap and the higher frequency of omission errors. The estimation of diameter at breast height showed a high level of concordance with reference values measured in the field, confirming the robustness of the method under different conditions. While tree height estimation was affected by limitations specific to terrestrial laser scanning, particularly due to occlusion effects, these limitations were reduced through the integration of UAV data. The analysis of relationship between radial growth, crown characteristics and competition highlighted the determinant role of crown dimensions in explaining radial growth variation, with crown length emerging as the main predictor, while crown diameter played a complementary role and the competition index had a lower contribution. At the same time, it was demonstrated that the effect of competition on radial growth is not exclusively direct, but is largely mediated through changes in crown dimensions, especially through the reduction of crown length. Moreover, the identified relationships vary depending on stand type, being more pronounced in mixed stands (spruce-beech) compared to pure stands (beech, spruce). The applied models confirmed the capacity of crown characteristics to explain the dynamics of radial growth. Overall, the results highlight the strong potential of integrating remote sensing data acquired from active and passive sensors for the determination of tree Dendrometric characteristics and for the analysis of radial growth.